Increased metabolism in combination with the novel cytochrome *b* target-site mutation L258F confers cross-resistance between the Q_o inhibitors acequinocyl and bifenazate in *Tetranychus urticae*

Running title: New Q_oI resistance mechanism in *T. urticae*

Xueping Lu [a], Marilou Vandenhole [a], Dimitra Tsakireli [b, c], Spiros A. Pergantis [d], John Vontas [b, c], Wim Jonckheere [a], Thomas Van Leeuwen [a,*]

[a] Laboratory of Agrozoology, Department of Plants and Crops, Faculty of Bioscience Engineering, Coupure Links 653, Ghent University, B-9000 Ghent, Belgium

[b] Laboratory of Pesticide Science, Department of Crop Science, Agricultural University of Athens, 75 Iera Odos Street, GR-11855 Athens, Greece

[c] Institute of Molecular Biology & Biotechnology, Foundation for Research & Technology, Hellas, 100 N. Plastira Street, GR-700 13 Heraklion, Crete, Greece

[d] Environmental Chemical Processes Laboratory, Department of Chemistry, University of Crete, Voutes Campus, 70013, Heraklion, Crete, Greece

* Corresponding author; thomas.vanleeuwen@ugent.be

ORCID of each author:

Xueping Lu:	0000-0002-6951-8065
Marilou Vandenhole:	0000-0002-4654-4498
Dimitra Tsakireli:	0000-0002-6213-9257
Spiros A. Pergantis:	0000-0002-9077-7870
John Vontas:	0000-0002-8704-2574
Wim Jonckheere:	0000-0001-8081-3500
Thomas Van Leeuwen:	0000-0003-4651-830X

Abstract

Acequinocyl and bifenazate are potent acaricides acting at the Q_o site of complex III of the electron transport chain, but frequent applications of these acaricides have led to the development of resistance in spider mites. Target-site resistance caused by mutations in the conserved cd1- and ef-helices of the Q_o pocket of cytochrome *b* has been elucidated as the main resistance mechanism. We therefore monitored Q_o pocket mutations in European field populations of *Tetranychus urticae* and uncovered a new mutation, L258F. The role of this mutation was validated by revealing patterns of maternal inheritance and by the independently replicated introgression in an unrelated susceptible genetic background. However, the parental strain exhibited higher resistance levels than conferred by the mutation alone in isogenic lines, especially for acequinocyl, implying the involvement of strong additional resistance mechanisms. This was confirmed by revealing a polygenic inheritance pattern with classical genetic crosses and via synergism experiments. Therefore, a genome-wide expression analysis was conducted that identified a number of highly overexpressed detoxification genes, including many P450s. Functional expression revealed that the P450 CYP392A11 can metabolize bifenazate by hydroxylation of the ring structure. In conclusion, the novel cytochrome *b* target-site mutation L258F was uncovered in a recently collected field strain and its role in acequinocyl and bifenazate resistance was validated. However, the high level of resistance in this strain is most likely caused by a combination of target-site resistance and P450-based increased detoxification, potentially acting in synergism.

Keywords: *Tetranychus urticae*; acequinocyl; cytochrome *b*; target-site mutation; Q_oI, Cytochrome P450, CYP392A11

1 Introduction

The phytophagous two-spotted spider mite *Tetranychus urticae* Koch (Acari: Tetranychidae) is a major cosmopolitan pest, infesting a broad variety of agricultural crops and causing huge economical loss when not controlled successfully (Jeppson et al., 1975). Although environmentally friendly methods and integrated pest management are becoming increasingly important in fields and greenhouses (van Lenteren et al., 2018), spider mites are still mainly controlled by synthetic acaricides due to their effectiveness, practicality and reasonable cost (Van Leeuwen et al., 2015). However, the intensive acaricide applications over the past decades led to the widespread evolution of acaricide resistance in mites. *Tetranychus urticae* has developed resistance to 96 active ingredients so far and is considered as one of the most resistant arthropods in the world (Mota-Sanchez and Wise, 2022; Van Leeuwen and Dermauw, 2016; Van Leeuwen et al., 2010). Maintaining *T. urticae* below economic injury levels is hence becoming increasingly challenging. To safeguard the efficacy and future use of the limited number of commercial products available, keeping resistance at bay is of utmost importance (Sparks et al., 2020). Successful resistance management strategies however require a comprehensive knowledge of the mechanisms by which the pest developed resistance (Hammock and Soderlund, 1986; Van Leeuwen et al., 2020).

An important target site for acaricides is the mitochondrial electron transport (MET) chain, located in the mitochondria, the power plants of the eukaryotic cell (D'Souza and Minczuk, 2018). The MET chain consists of four large transmembrane enzyme complexes (Complex I-IV), which together transfer electrons from NADH and succinate to molecular oxygen (D'Souza and Minczuk, 2018; Lümmen, 2007). This electron flow is coupled to the transport of protons across the inner mitochondrial membrane. Flowing back into the mitochondrial matrix via the ATP synthase complex, these protons eventually drive the production of ATP (D'Souza and Minczuk, 2018; Flampouri, 2021). Within the MET chain, complex III, also

known as ubihydroquinone:cytochrome c oxidoreductase or *bc1* complex, catalyzes the electron transfer from reduced ubiquinone to cytochrome *c* (Lümmen, 2007). Complex III has three core subunits that are highly conserved from bacteria to mammals: cytochrome *b* (*cytb*), cytochrome c_1, and the Rieske iron-sulfur protein (D'Souza and Minczuk, 2018; Yang and Trumpower, 1986). Importantly, cytochrome *b* is the only complex III subunit that is mitochondrially encoded (D'Souza and Minczuk, 2018). Cytochrome *b* harbors two distinct quinone-binding sites, Q_i and Q_o, located near the inner and outer sides of the inner mitochondrial membrane, respectively (D'Souza and Minczuk, 2018; Di Rago and Colson, 1988; Xia et al., 1997). Inhibitors targeting these sites, hence inhibiting respiration, are known as quinone inside inhibitors (Q_iI) and quinone outside inhibitors (Q_oI) (Di Rago et al., 1989; Flampouri, 2021). Several bacterial and fungal metabolites acting as inhibitors are known (Bartlett et al., 2002; Di Rago and Colson, 1988; Sauter et al., 1999), yet also in plants such inhibitors can be found (Khambay et al., 1997). Next to the existence of natural inhibitors, synthetic inhibitors have been developed. An example of such synthetic Q_oI is acequinocyl, a naphthoquinone miticide discovered in the 1970s by DuPont and commercialized in 1999 by Agro Kanesho (Bellina and Fost, 1977; Dekeyser, 2005; Wakasa and Watanabe, 1999). It is a pro-acaricide that needs to be activated to its toxic deacetylated metabolite (Caboni et al., 2004; Dekeyser, 2005). The mode of action was identified by Koura et al. (1998), who observed that the deacetylated metabolite of acequinocyl inhibited the respiration of mitochondria at complex III in house fly flight muscles. More than a decade later, the second synthetic Q_oI, the hydrazine carbazate bifenazate, was commercialized (Grosscurt and Avella, 2005). It was also shown to be a pro-acaricide, requiring *in vivo* activation by carboxyl/cholinesterases (Van Leeuwen et al., 2006). It is thought that the principal active metabolite is the diazene, and an activation pathway was suggested (Ochiai et al., 2007; Van Leeuwen et al., 2006). Bifenazate was first thought to act as a neurotoxic compound targeting the GABA receptors (Dekeyser, 2005), until investigation

104 of the resistance mechanisms in spider mites provided strong genetic evidence for cytochrome
105 *b* as the target site ((Van Leeuwen et al., 2008); reviewed in (Van Leeuwen et al., 2015)).

106 Acaricide resistance is predominantly the result of direct changes to the proteins that are the
107 target site of the acaricide (pharmacodynamic mechanisms) or by enhancing the metabolic
108 ability of the enzymes, quantitatively or qualitatively, that modify the acaricide itself before it
109 reaches its target (pharmacokinetic mechanisms) (Feyereisen et al., 2015). A number of
110 detoxifying enzymes and transporters have been characterized and implicated in resistance in
111 *T. urticae*, including carboxyl/cholinesterases, glutathione-S-transferases, P450 mono-
112 oxygenases, ABC-transporters and members of the Major Facilitator Family (Van Leeuwen and
113 Dermauw, 2016). A number of horizontally transferred genes have also largely increased the
114 metabolic potential of *T. urticae*, such as UDP-glycosyltransferases (UGTs) and intradiol-ring
115 cleaving dioxygenases. The latter family was recently shown to cleave the aromatic ring
116 structures of many mono- and polycyclic plant defense compounds (Njiru et al., 2022). In
117 several resistance cases, pharmacodynamic and pharmacokinetic mechanism work together,
118 which may result in additive or even synergistic effects (De Beer et al., 2022; Snoeck et al.,
119 2019; Wybouw et al., 2019).

120 The main molecular mechanism associated with acequinocyl and bifenazate resistance in spider
121 mites of the genera *Tetranychus* and *Panonychus* are mutations in conserved regions in the *cytb*
122 Q_o pocket. To date, six such mutations or mutation combinations have been discovered in *T.*
123 *urticae* (last reviewed in (Fotoukkiaii et al., 2020b)). Their contribution to acequinocyl and
124 bifenazate resistance in *T. urticae* has been elucidated by revealing maternal inheritance in
125 reciprocal crosses and by repeated backcrossing experiments to introduce the mutation in a
126 different nuclear genetic context (Fotoukkiaii et al., 2020b; Kim et al., 2019; Riga et al., 2017;
127 Van Nieuwenhuyse et al., 2009). Single mutations in the Q_o pocket, identified so far, are G132A
128 (cd1-helix) and P262T (ef-helix). In other cases, a combination of two mutations was found in

129 the resistant strains, such as G126S in combination with A133T, I136T or S141F (all in the cd1-
130 helix) (Fotoukkiaii et al., 2020b; Van Leeuwen et al., 2008). However, the G126S mutation
131 alone does not confer bifenazate nor acequinocyl resistance, and is likely a neutral
132 polymorphism (Xue et al., 2021). Whether or not the other substitutions in the combinations
133 confer resistance by themselves, or require the presence of G126S, remains unknown and is not
134 straightforward to investigate. Indeed, uncoupling of mutations in mitochondrial DNA, where
135 recombination is absent, is not possible, and these single mutations remain to be detected in the
136 field.

137 The frequency of these known mutations and the detection of potentially new *cytb* mutations in
138 the field remains crucial for resistance monitoring and for designing reliable molecular markers
139 (Van Leeuwen et al., 2020). Therefore, we monitored the *cytb* genotype in European field
140 populations, leading to the discovery of a new mutation, whose contribution in resistance to
141 both acequinocyl and bifenazate was studied.

142 # 2 Material and methods

143 ## 2.1 Mites and chemicals

144 For the *cytb* screening, 30 field populations (FP1-FP30) were collected from different locations
145 across Europe between 2018 and 2020 (**Table S1** and **Fig. 1**). In addition, we used the
146 susceptible lab strain London (LON) as a reference (Khajehali et al., 2011). Mites were raised
147 on bean plants, *Phaseolus vulgaris* L. cv. 'Prelude', in a climate chamber at 25±1°C, 60%
148 relative humidity and a 16:8 h light:dark photoperiod. Field population 9 (FP9) was maintained
149 on bean leaves sprayed with 200 mg/L acequinocyl.

150 Commercially formulated acequinocyl (Cantack®, Certis, 164 g/L SC) and bifenazate
151 (Floramite®, Bayer, 240 g/L SC) were purchased from Intergrow (Aalter, Belgium). All other
152 chemicals were purchased from Sigma-Aldrich (Belgium) except when mentioned otherwise.

153 **2.2 Survey of *cytb* genotypes**

154 DNA extractions and PCRs were conducted as described previously (Van Leeuwen et al., 2008).
155 Approximately 200 adult female mites per population were used in the extractions. Primers are
156 provided in **Table S2** (Khajehali et al., 2011). The acquired sequencing data were further
157 analyzed using SeqMan and BioEdit (Hall, 1999), and deposited into the NCBI repository
158 database. The sequences are available in GenBank with accession numbers OP797802 to
159 OP797832. Sequencing chromatographs were visually inspected for the presence of segregating
160 mutations, which allows to reliably detect mutations at frequencies higher than 10-20% (Van
161 Leeuwen et al., 2008; Xue et al., 2022).

162 **2.3 Toxicity bioassays**

163 Adulticidal bioassays were performed to evaluate the toxic effects of acequinocyl and
164 bifenazate, as described previously (Khajehali et al., 2011). The dose-response relationships
165 (lethal concentration 50 with 95% confidence interval) were determined by probit regression
166 analysis using Polo Plus version 2.0 (LeOra software, Berkeley, CA, USA) (Robertson and
167 Preisler, 1992).

168 Acequinocyl-hydroxy was dissolved in a mixture of N,N-dimethylformamide and emulsifier W
169 (alkylarylpolyglycolether), 3:1 w:w, respectively, and diluted with deionized water 100-fold
170 before being used in bioassays.

171 **2.4 Inheritance of resistance**

172 To determine the inheritance pattern of the observed acequinocyl and bifenazate resistance of
173 FP9, reciprocal crosses were established between FP9 and the susceptible reference LON, as
174 described previously (Van Leeuwen et al., 2004). Briefly, 260 virgin females from each strain
175 were paired with 260 mature males of the other strain by placing them on the upper side of bean
176 leaf discs on wet cotton in Petri dishes and allowing them to mate for two days. The females
177 were then collected and transferred to fresh bean leaves for oviposition. The resulting F1

178 females (1-3 days old adults) were used for toxicity bioassays as described above, with
179 concentrations covering the range of 0-100% mortality.

180 Dominance or recessivity of the resistance was estimated by the formula of Stone (1968), in
181 which the dominance (D) is given by $D = (2X_2 - X_1 - X_3)/(X_1 - X_3)$, where $X_1 = \log LC_{50}$ of the
182 homozygous resistant strain (FP9, genotype R), $X_2 = \log LC_{50}$ of the heterozygous female F1
183 progeny from each reciprocal cross (genotype RS and SR) and $X_3 = \log LC_{50}$ of the homozygous
184 susceptible strain (LON, genotype S). A value of -1 indicates fully recessive inheritance, 0
185 represents neither dominance nor recessivity, and +1 indicates fully dominant inheritance.

186 Next, around 400 F_1 heterozygous virgin females from the reciprocal cross ($R^{♀}\times S^{♂}$) were
187 allowed to mate with FP9 males ($RS^{♀}\times R^{♂}$) on bean leaves for two days, as mentioned above.
188 The resulting F_2 females (1-3 days old adults) were then subjected to toxicity bioassays.
189 Monogenic or polygenic inheritance was determined by the methods provided by Georghiou,
190 and included a visual inspection for a plateau at 50% mortality in the concentration-mortality
191 curve of the F_2 females (Georghiou, 1969). The expected response of monogenic F_2 females at
192 a given concentration was calculated using the following formula: $c = (0.5)\ W_{RS} + (0.5)\ W_{RR}$,
193 where W is the observed mortality of the RS and RR genotypes at that given concentration
194 (Georghiou, 1969). The χ^2-goodness of fit test was then used to evaluate the hypothesis of
195 monogenic inheritance (Van Pottelberge et al., 2009a). Dose-response curves were constructed
196 using Sigmaplot (Version 14.5).

197 **2.5 Construction of isogenic lines via repeated backcrossing**

198 To uncouple the L258F mutation in the G126S background from other nuclear encoded
199 resistance loci, introgressed lines were generated using the marker-assisted backcrossing
200 method described by Bajda et al. (2017). Briefly, a virgin female of FP9 was crossed with a
201 haploid male of the LON strain (without the mutations) ($R^{♀}\times S^{♂}$). The resulting virgin female
202 was backcrossed to a LON male ($RS^{♀}\times S^{♂}$). This backcrossing was repeated for eight

generations. In the last generation, a mother-son cross was carried out to produce a near-isogenic line (NIL) carrying the mitochondrially encoded mutation combination (as verified by *cytb* sequencing) in a nuclear genome background mostly originating from the susceptible LON strain. This backcrossing experiment was performed in three biological replicates, resulting in three independent near-isogenic lines. Dose-response curves were depicted using Sigmaplot (Version 14.5).

2.6 Synergism/antagonism experiments

Synergism/antagonism experiments were conducted as described previously (Khalighi et al., 2014; Van Pottelberge et al., 2009b). Briefly, 1000 mg/L of the cytochrome P450 monooxygenase enzyme inhibitor piperonyl butoxide (PBO), 500 mg/L of the general esterase enzyme inhibitor S,S,S-tributyl phosphorotrithioate (DEF) (ChemService, USA), 2000 mg/L of the glutathione S-transferase enzyme inhibitor diethyl maleate (DEM), or blank formulation, were used to treat females. After 24 h, the surviving mites were transferred to new leaf discs and used for toxicity experiments as mentioned above. LC_{50} values, synergism ratios (SR), resistance ratios (RR) and corresponding 95% confidence intervals (CI) were calculated using PoloPlus. The SRs were calculated as the acequinocyl LC_{50} after blank pre-treatment relative to the LC_{50} value after synergist pre-treatment.

2.7 RNA extraction and sequencing

To examine genome-wide gene expression patterns associated with acequinocyl resistance, RNA sequencing experiments were performed. Total RNA was extracted from pools of 100-120 adult female mites using the RNeasy plus mini kit (Qiagen, Belgium) with four biological replicates for LON, FP9 mites under continuous acequinocyl exposure ($FP9_{ace}$) and FP9 mites taken off acequinocyl selection pressure for one generation time ($FP9_{unexp}$). Both quality and quantity parameters of the resulting total RNA were checked using a DeNovix DS-11 spectrophotometer (DeNovix, USA) as well as via visual inspection of the integrity on a 1%

agarose gel. From these RNA samples, Illumina libraries were constructed with the Illumina TruSeq Stranded mRNA Library Preparation Kit, and the resulting libraries were subsequently sequenced using the Illumina NovaSeq6000 technology to generate an output of stranded paired reads of 2 × 100 bp (library construction and sequencing was performed at Macrogen Europe, Amsterdam, The Netherlands).

2.8 RNA mapping and PCA

The quality of the RNA reads was verified using FASTQC (version 0.11.9) (Andrews, 2010). The RNA reads of samples that passed the quality control were aligned to the *T. urticae* three-chromosome genome assembly using the two-pass alignment mode of STAR (version 2.7.9a) with a maximum intron size set to 20 kb (Dobin et al., 2013; Wybouw et al., 2019). Resulting BAM files were subsequently sorted by chromosomal coordinate and indexed using SAMtools (version 1.11) (Li et al., 2009). HTSeq (version 0.11.2) was used to perform read-counting on a per-gene basis with the default settings and *--stranded yes* and *--feature exon* (Anders et al., 2015). These count files were used as an input for the R-package (R version 4.2.0) DESeq2 (version 1.36.0) to perform a PCA analysis in order to research gene expression variation within and between the three treatment groups LON, $FP9_{unexp}$ and $FP9_{ace}$. Briefly, the counts were normalized via the regularized-logarithm (rlog) transformation function of the DESeq2 package and the PCA was calculated and plotted for the 5000 most variable genes across all RNA samples using the DESeq2 function PlotPCA (Love et al., 2014).

2.9 Differential gene expression analysis

Differential expression (DE) analysis was performed using DESeq2 (version 1.36.0) based on the total per-gene read counts generated by HTSeq (see above) (Love et al., 2014). In first instance, gene expression changes associated with acequinocyl and bifenazate resistance was assessed by identifying significantly differentially expressed genes (DEGs, Log_2 Fold Change (Log_2FC) > |1|, Benjamini-Hochberg adjusted p-value <0.05) in the $FP9_{unexp}$ vs LON and $FP9_{ace}$

253 vs LON comparisons (Benjamini and Hochberg, 1995). To assess the extra effect of continuous
254 acequinocyl induction, the same method was used to identify DEGs in the $FP9_{ace}$ vs $FP9_{unexp}$
255 comparison. A Venn diagram representing the overlap of differentially expressed genes in all
256 contrasts was made using the R package VennDiagram. From these lists of DEGs, subsets of
257 genes belonging to important detoxification families were made (Kurlovs et al., 2022). A
258 volcanoplot, color coded by detoxifying gene family, and a shared overexpression plot were
259 produced with the ggplot2 (version 3.3.6) package (Wickham, 2016).

260 **2.10 Gene ontology (GO) enrichment analysis**

261 The R function "enricher" from the package clusterProfiler v4.2.2 was used for GO enrichment
262 analysis. The GO terms for Biological Processes (BP) and Molecular Functions (MF) were
263 collected based on the *T. urticae* annotation (version 20190125) from the Orcae database
264 (Sterck et al., 2012). Multiple correction was performed using a Benjamini-Hochberg procedure
265 by assigning the argument "pAdjustMethod = 'BH'".

266 **2.11 Functional expression of CYP392A11 and bifenazate metabolism**

267 Because of its high upregulation in FP9, the P450 CYP392A11 (*tetur03g00970*) was selected
268 from the differential expression analysis for functional validation of its potential role in
269 bifenazate metabolism. The analytical method for acequinocyl and acequinocyl-OH
270 quantification was not reproducible in our hands and thus we could not examine the potential
271 role of CYP392A11 in acequinocyl metabolism. Preparation of bacterial membranes co-
272 expressing CYP392A11 with *T. urticae* cytochrome P450 reductase (CPR) was performed as
273 described in Riga et al. (2015). Stock concentrations of bifenazate (100 % purity, Sigma Aldrich)
274 were prepared and diluted in acetonitrile. Standard reactions contained a final organic solvent
275 concentration of 2.5 % (v/v) with 25 µM of bifenazate and 25 pmol of CYP392A11 bacterial
276 membranes in 100 µl Tris-HCl buffer (0.2 M, pH 7.4), containing 0.25 mM $MgCl_2$. The
277 incubation was performed in the presence and absence of an NADPH generating system: 1 mM

glucose-6-phosphate (Sigma Aldrich), 0.1 mM $NADP^+$ (Sigma Aldrich) and 1 unit/ml glucose-6-phosphate dehydrogenase (G6PDH; Sigma Aldrich). Reactions were incubated at 30 °C, 1250 rpm oscillation and stopped at 0 and 2 hour time points by adding 100 µl acetonitrile and stirring the mixture for an additional 30 min. Finally, the quenched reactions were centrifuged at 10,000 rpm for 10 min and the supernatant was transferred to HPLC vials, with 100 µl of the supernatant loaded for HPLC analysis. Reactions were performed in triplicate and compared against a negative control without NADPH regenerating system to calculate substrate depletion. Bifenazate was separated on a 3 µm C18 (100 × 2.1 mm) reverse phase analytical column (Fortis). Reactions with bifenazate were separated using an isocratic mobile phase of 10% H_20 and 90% acetonitrile with a flow rate of 0.1 ml/min for 5 min. Reactions were monitored by changes in absorbance at 231 nm, and bifenazate quantified by peak integration and standard curve (Chromeleon, Dionex).

2.12 Identification of reaction products of bifenazate by HPLC-MS analysis

The reactions of the P450 CYP392A11 enzyme with bifenazate in the presence and absence of an NADPH generating system were further analyzed using high-resolution HPLC-MS/MS system. Sample injections (1 µl loop) were performed via an Ultimate 3000 Autosampler (Thermo Scientific, USA). Chromatographic separation was achieved using an Ultimate 3000 (Thermo Scientific, USA), equipped with a 3 µm C18 (100 x 2.1 mm) reverse phase analytical column (Fortis). An isocratic mobile phase of 10% H_20 and 90% acetonitrile with a flow rate of 0.1ml/min for 5 min. Analyte detection was achieved using an electrospray ionization (ESI) Q Exactive Hybrid Quadrupole-Orbitrap Mass Spectrometer (Thermo Scientific, USA), operated in the positive ion mode. Mass spectrometry was operated both in full scan/extracted ion monitoring and parallel reaction monitoring (PRM). The system was controlled by the Xcalibur software, which was also used for data acquisition and analysis. The optimum mass spectrometer parameters were set as follows: spray voltage at 3500V, sheath gas pressure at 20

arbitrary units, auxiliary gas pressure at 10 arbitrary units, ion transfer capillary temperature at 250 ^{0}C. In the parallel reaction monitoring, the source collision induced dissociation at 30 eV. Sheath/aux and collision gas was high purity nitrogen.

3 Results

3.1 Cytochrome *b* genotype screening

Monitoring of *cytb* Q_o genotypes in European field populations of *T. urticae* identified two previously reported substitutions (G132A and P262T) and the novel substitution L258F (A to T transversion at position 774) (**Fig. 1** and **Fig. 2**). This novel mutation was found on the 126S haplotype and was only detected in a population from the Netherlands (i.e. FP9), in which the mutation appeared to be fixed. The G132A and P262T mutations were each found to be segregating in a population from Belgium. The neutral G126S substitution, without additional substitutions, was found in 3 out of 30 field populations.

3.2 Mode of inheritance of acequinocyl and bifenazate resistance

The results from the experiments investigating the mode of inheritance of acequinocyl and bifenazate resistance in FP9 are presented in **Table 1** and **Fig. 3 panel A and B**.

A clear maternal inheritance was detected for both acequinocyl and bifenazate resistance, as the 95% CI of the LC_{50} for F1 females from the reciprocal crosses SR (S♀ x R♂) and RS (R♀ x S♂) did not overlap while the degree of dominance differed depending on the direction of the cross (**Table 1**). This also becomes clear from visual inspection of the concentration-mortality curves from these reciprocal crosses (**Fig. 3 panel A and B**), with the SR curve positioned close to the curve of the susceptible reference LON, and the RS curve positioned intermediate between both parental strains. This clearly indicates that a part of the resistance phenotype is maternally inherited and most likely linked to the mitochondrial mutation L258F in *cytb*.

In an attempt to estimate the number of genes involved, the backcross experiment for acequinocyl showed a significant difference (χ^2 = 108.67, df = 16, *P*-value < 0.05) between the observed mortalities and the mortalities expected for monogenic resistance at tested concentrations (**Fig. 3 panel A**), suggesting that more than one gene was involved in resistance. In addition, no plateau was observed at the 50% mortality level of the backcross generation, also indicating resistance was not the responsibility of a single gene (Georghiou, 1969).

3.3 Contribution of L258F to the resistance

Introgression lines, carrying the novel mutation L258F on the 126S haplotype in a susceptible nuclear genomic background (LON strain) validated the mutation, but also showed a largely decreased level of resistance to acequinocyl (RR of 6.1-fold) and bifenazate (RR of 22-fold), compared to the resistant FP9 (RR of 290 and 150 respectively) (**Table 1** and **Fig. 3 panel C and D**).

3.4 Toxicity of the active acequinocyl-hydroxy metabolite

While the LON strain showed an increased susceptibility to the active metabolite acequinocyl-HO (LC_{50} of 1.7 mg L^{-1}) relative to acequinocyl (LC_{50} of 9.6 mg L^{-1}), the susceptibility of FP9 to the metabolite remained low (LC_{50} > 2000 mg L^{-1}), relative to acequinocyl (LC_{50} of 2700 mg L^{-1}). As such, the RR for acequinocyl-OH (>1200-fold) increased compared to that of acequinocyl (290-fold) (**Table 2**). It therefore seems unlikely that reduced activation of acequinocyl into acequinocyl-OH contributes to resistance.

3.5 Synergism or antagonism experiments

Both PBO, DEF and DEM significantly synergized acequinocyl toxicity in FP9. Synergism was strongest for PBO (SR of 11-fold), relative to DEF (7.3-fold) and DEM (2.6-fold) (**Table 3**). In LON, pre-treatment with PBO did not significantly affect the acequinocyl toxicity. DEF and DEM pre-treatment, however, appeared to have a small, yet significant, antagonistic effect, with SRs of 0.74- and 0.89-fold, respectively (**Table 3**).

3.6 RNAseq and principal component analysis (PCA)

The genome-wide gene expression patterns associated with acequinocyl resistance were examined using RNAseq, comparing three groups: LON, $FP9_{ace}$ and $FP9_{unexp}$. Illumina sequencing generated ~31 million strand-specific paired-end reads per sample of which an average of 81.7% mapped uniquely against the *T. urticae* three chromosome reference assembly (**Table S3**) (Wybouw et al., 2019). The RNA reads were deposited in the NCBI Sequence Read Archive under Bioproject (PRJNA946758) and raw read count data was made available on Figshare (10.6084/m9.figshare.22316929). Normalized read-counts of the 5000 most variable genes across all RNA samples were used to perform a PCA analysis (**Fig. 4 panel A**). The first two principal components cumulatively explained 90% of the variance; with PC1 accounting for 85% of the total variance and PC2 for 5%. The $FP9_{unexp}$ replicates clustered together with the $FP9_{ace}$ replicates, indicating only little expression variation between both groups. In addition, both were well separated from the LON samples along PC1. The clustering of the sample replicates confirmed their quality.

3.7 Differential gene expression analysis

A total of 2374 and 2355 genes were differentially expressed when comparing $FP9_{unexp}$ and $FP9_{ace}$ to LON, respectively. The majority of the differentially expressed genes (72.95 %) was shared between $FP9_{unexp}$ and $FP9_{ace}$, of which 1166 genes were significantly upregulated and 824 downregulated in both groups (**Fig. 4 panel B**). For $FP9_{unexp}$, the top 20 overexpressed genes ranged from Log_2FC 9.25 to 12.49, whereas the top 20 downregulated genes ranged from Log_2FC -8.45 to -10.35 (**Table S4**). As shown in **Fig. 4 panel C**, which represents a volcano plot of the $FP9_{unexp}$ vs LON comparison, a large fraction of DEGs belongs to various detoxifying gene families. Amongst some of the highest expressed genes, there are several genes coding for short chain dehydrogenases *(tetur06g04960, tetur06g04970, tetur511g00010*), with *tetur06g04970* being the most highly upregulated one (log_2 FC of 12.22), an intradiol ring-

cleavage dioxygenase (*tetur07g06560*), a carboxyl/cholinesterase pseudogene (*tetur24g02580*) and several cytochrome P450s like CYP392D2 (*tetur03g04990*), CYP385C3v2 (*tetur46g00170*), CYP392A11 (*tetur03g00970*), and some CYP pseudogenes (*tetur03g05020, tetur03g05110*). For $FP9_{ace}$, the top 20 overexpressed genes ranged from Log_2FC 9.32 to 13.09, amongst which 15 are shared with $FP9_{unexp}$ (**Table S4**). Interestingly, as shown in the overexpression plot for $FP9_{unexp}$ and $FP9_{ace}$ versus LON (**Fig. 4 panel C)**, a large shared number of DEGs is located along the diagonal of the axes, indicating a similar magnitude of Log_2FC for these genes in each treatment group. Moreover, when comparing $FP9_{ace}$ vs $FP9_{unexp}$ to study the effect of acequinocyl induction, only 71 genes were differentially expressed, with moderate Log_2FC values ranging from -5.43 to 2.73. This demonstrates that acequinocyl exposure only has a minor effect on gene expression in the resistant strain. Nevertheless, amongst the highest upregulated genes by acequinocyl induction ($FP9_{ace}$ versus $FP9_{unexp)}$, we find on top CYP392E10 (*tetur27g01030*) with a Log2FC of 2.73, but also a GST (TuGSTm10; *tetur05g05270*), and a UGT (*tetur05g09325*).

3.8 Gene ontology (GO) enrichment analysis

Based on our datasets of differentially expressed genes for each contrast, we have performed a GO enrichment analysis which is shown in **Table 4.** For the Biological Process (BP) subontology we have found 10 GO categories enriched in the $FP9_{unexp}$ group, of which eight were also enriched in the $FP9_{ace}$ group, whereas no BP GO terms were significantly enriched for $FP9_{ace}$ vs $FP9_{unexp}$. The Biological Process GO terms “proteolysis” (GO:0006508), “regulation of catalytic activity” (GO:0050790) and “oxidation-reduction process” (GO:0055114) can be considered the most important ones as they are enriched with the most significant adjusted p-values and the highest gene ratios. When taking a closer look at the genes associated with these GO terms, within “proteolysis” (GO:0006508) mainly cathepsins, peptidases and serine proteases can be found, whereas in “regulation of catalytic activity”

401 (GO:0050790) only cathepsin genes are found. To the category “oxidation-reduction process”
402 (GO:0055114) belong a lot of upregulated DOGs (8/92) and P450s (37/92).

403 For the Molecular Function (MF) subontology we found 18 GO categories enriched across
404 experimental groups. Two MF GO groups are strongly significant enriched for all treatment
405 groups, “cysteine-type peptidase activity” (GO:008234), which contains many cathepsins, and
406 “iron ion binding” (GO:0005506) which is composed of DOGs and P450s. Moreover, for
407 $FP9_{unexp}$ and $FP9_{ace}$ versus LON, three extra GO terms, “oxidoreductase activity, acting on
408 paired donors, with incorporation or reduction of molecular oxygen” (GO:0016705), “cysteine-
409 type endopeptidase activity” (GO:0004197) and transferase activity, transferring hexosyl
410 groups (GO:0016758) are enriched with highly significant p-values. Interestingly, apart from
411 cathepsin-, DOG- and P450-related GO terms, “transferase activity, transferring hexosyl groups”
412 (GO:0016758) has many UGT genes associated to it, amongst which several, e.g.
413 *tetur22g00360*, appeared to be highly upregulated (Log_2FC 6.44).

414 **3.9 CYP392A11 hydroxylates bifenazate**

415 Based on the differential expression analysis, one of the most highly upregulated P450s in the
416 resistant strain FP9, *CYP392A11* (Log_2FC of 7.59 for $FP9_{unexp}$) was selected for functional
417 expression to test its ability to metabolize bifenazate. The catalytic activity of the P450 was
418 assessed by measuring acaricide turnover in the presence and absence of NADPH and analyzing
419 the formation of metabolites. Incubation of the CYP392A11 complex with bifenazate for 2 h
420 revealed a 43.5% NADPH-dependent depletion of bifenazate (eluting at 4.9 min) and the
421 parallel formation of an unknown metabolite, M1 (**Fig. 5**). Metabolite M1 eluted at 4.075 min,
422 in the sample containing NADPH, while no metabolite was detected in the control without
423 NADPH.

424 HPLC-MS and MS/MS analysis of the reaction mixtures pointed towards hydroxylation as the
425 likely mechanism of the reaction catalyzed by CYP392A11. The accurate mass HLPC-MS

analysis confirmed the generation of hydroxy-bifenazate as the major detectable metabolite (**Fig. S1**). The positive ion mode mass spectrum of the bifenazate metabolite M1 showed the molecular ion peak at m/z $[M + H]^+$ =317.1496, which is 16 m/z units higher than the corresponding peak in the spectrum of the parent compound at m/z $[M + H]^+$ =301.1549. Accurate mass measurements showed that the +16 Da corresponds to an O atom, implying the hydroxylation reaction. The MS/MS spectra of the parental bifenazate and its metabolite shows a fragmentation pattern that corresponds to hydroxylation occurring on the aromatic system, with several hydroxylation sites being possible (**Fig. 6**). This is supported by the fact that all bifenazate fragments containing the aromatic system, shift upwards by 16 Da in the corresponding M1 metabolite fragments ions.

4 Discussion

The Q_oI acaricides bifenazate and acequinocyl have been used as efficient and selective acaricides for more than a decade, and are still frequently used today (Dekeyser, 2005; Grosscurt and Avella, 2005; Van Leeuwen et al., 2015; Wakasa and Watanabe, 1999). However, due to their frequent use as selective acaricides, resistance has emerged (Fotoukkiaii et al., 2020b; Kim et al., 2019; Van Leeuwen et al., 2011; Van Leeuwen et al., 2008; Van Nieuwenhuyse et al., 2009). Over the years, a number of Q_o mutations (G132A, A133T, S141F, I260V, and P262T) conferring bifenazate and/or acequinocyl resistance have been uncovered and validated by revealing a maternal inheritance pattern. Additionally, the phenotypic strength of some Q_o mutations has been determined by repeated back-crossing into a susceptible population (**Table S5**). Because of the strong causal correlation between the presence of Q_o mutations and Q_oI resistance (Fotoukkiaii et al., 2020b; Kim et al., 2019; Riga et al., 2017; Van Leeuwen et al., 2011; Van Leeuwen et al., 2008), we sequenced the complete *cytb* of a collection of field strains as a first step in searching for reliable molecular markers for field resistance monitoring in Europe (Van Leeuwen et al., 2020). We took advantage of the available

DNAs of a set of field-collected strains from a study screening for abamectin resistance (Xue et al., 2020). The *cytb* genotyping data of this study first revealed that the incidence of known target-site resistance mutations was relatively low, as they were only identified in two out of thirty (7%) screened populations. This is consistent with a previous recent monitoring study conducted by Fotoukkiaii et al. (2020b). However, our field monitoring also led to the discovery of a novel mutation, L258F at the boundary of the highly conserved ef-helix of *cytb* in strain FP9 from the Netherlands. Toxicity assays subsequently confirmed that this strain was resistant to both acequinocyl and bifenazate. The mutation occurred on the 126S haplotype and is in close proximity of a substitution (P262T) for which involvement in resistance is very well supported (Kim et al., 2019; Riga et al., 2017; Van Leeuwen et al., 2008; Van Nieuwenhuyse et al., 2009). The G126S mutation alone does not confer bifenazate nor acequinocyl resistance, and is likely a neutral polymorphism segregating in many populations (Xue et al., 2021). It is therefore not clear whether there is any additional effect of the combination of G126S and L258F, or whether this mutation just arose by chance on the 126S *cytb* haplotype. This might also be the case for previously reported mutation combinations (see **Table S5** and **Fig. 2**). As recombination does not occur in animal mitochondria (Ladoukakis and Zouros, 2017; Scheffler, 2001), experimentally separating both mutations via recombination, i.e., through crossing, is not feasible.

Reciprocal crosses between the resistant FP9 and the susceptible LON strain revealed that the acequinocyl and bifenazate resistance was in part maternally inherited, providing evidence for the involvement of the mitochondrially encoded *cytb* target site mutation L258F. However, this experiment also showed that maternal inheritance was far from complete, in contrast to what has been documented for other *cytb* resistance mutations (Fotoukkiaii et al., 2020b; Kim et al., 2019; Van Leeuwen et al., 2006; Van Leeuwen et al., 2011; Van Nieuwenhuyse et al., 2009). This strongly suggests the presence of additional resistance mechanisms. Introgression

476 experiments are a good experimental tool to further corroborate the presence of additional
477 mechanisms and to investigate their relative importance (Riga et al., 2017) (see **Table S5** for
478 *cytb* mutations). Introgression experiments showed that the phenotypic effect of L258F in an
479 isogenic susceptible background results in relatively low levels of resistance to acequinocyl and
480 bifenazate. The phenotypic effect of L258F is also much less compared to the nearby P262T
481 mutation (Table S5). The presence of additional mechanisms is most clear for acequinocyl,
482 where the mutation causes about 6-fold resistance, compared to 290-fold in the field-collected
483 FP9. Indeed, backcrossing experiments (RS♀×R♂) did not support a monogenic model for
484 acequinocyl inheritance, further corroborating the presence of additional mechanisms.

485 The involvement of additional factors in resistance was first investigated using synergist assays,
486 as this is a straightforward method to identify the involvement of major metabolic pathways in
487 both toxicity and resistance mechanisms (De Beer et al., 2022; Fotoukkiaii et al., 2020a;
488 Fotoukkiaii et al., 2021; Snoeck et al., 2019; Van Pottelberge et al., 2009b). A slight antagonism
489 of toxicity was found after treatment with DEF and DEM for the LON strain, which supports
490 that acequinocyl needs to be hydrolytically activated in *T. urticae* (Dekeyser, 2005), similar as
491 what has been reported for bifenazate (Sugimoto and Osakabe, 2019; Van Leeuwen et al., 2006).
492 Decreased activation of a pro-acaricide to its active metabolite is a potential resistance
493 mechanism (David, 2021), as was recently reported for high coumaphos resistance levels in
494 *Varroa* (Vlogiannitis et al., 2021). If a similar mechanism of decreased activation exists in FP9,
495 the resistance is expected to be lower for the activated metabolite compared to acequinocyl
496 itself, as the *in vivo* activation step is bypassed by applying the active metabolite directly. By
497 comparing toxicity data between acequinocyl and its active metabolite for FP9 and LON, it was
498 shown that there is no reduced activation in the resistant FP9. In contrast, PBO, DEF and DEM
499 all had a significant negative effect on the LC_{50} of acequinocyl in the resistant population.
500 Therefore, increased metabolism is most likely an additional resistance mechanism and

especially cytochrome P450 monooxygenases and CCEs seem to be important. This is consistent with the former observation that either PBO and DEF, or both, enhanced acequinocyl toxicity in resistant strains (Kim et al., 2019; Sugimoto and Osakabe, 2019; Van Nieuwenhuyse et al., 2009; Yorulmaz Salman and Sarıtaş, 2014).

As synergism experiments only give a general idea of which detoxification families contribute to the observed resistance, we proceeded with a genome-wide gene expression analysis between the susceptible LON strain and FP9 that was either exposed to acequinocyl ($FP9_{ace}$) or was left unexposed (FP_{unexp}). We included the latter treatment, as theoretically, increased induction could be a resistance mechanism, and this is usually overlooked when examining gene expression without exposure. Both comparisons are needed to get a full understanding of potential mechanisms, as, on the other hand, comparing exposed mites to a non-exposed control might only reveal induced genes that might not contribute to resistance. There was only a very limited set of genes differentially expressed between exposed and non-exposed mites of the resistant strain (**Fig. 4 panel B**), and it is clear that acequinocyl does not mount a strong response in FP9. Interestingly, CYP392E10 is the highest upregulated gene in the comparison FP9 exposed versus non-exposed, whereas this was the most extreme downregulated gene in the comparison of FP9 vs LON. Thus, for FP9, CYP392E10 upregulation seems dependent on acequinocyl exposure. Similarly, CYP392E10 was strongly induced upon spirodiclofen exposure and was shown to metabolize spirodiclofen by hydroxylation (Demaeght et al., 2013; Wybouw et al., 2019). However, since induction data of acequinocyl on the LON strain was not available, it is not clear whether this induction contributes to resistance.

We then further focused on the comparison of constitutive differences between resistant and susceptible populations, and this expression analysis identified genes belonging to the detoxification families of the SDRs, cytochrome P450s, DOGs and CCEs amongst the highest upregulated genes in FP9. Given the observed large transcriptional response, it is likely that

field selection to resistance resulted in altered trans regulatory mechanisms. Indeed, trans regulation of detoxifying enzymes is very common in *T. urticae*, especially for P450s, as was recently documented in a seminal study using a panel of inbred *T. urticae* strains using allele-specific expression data (Kurlovs et al., 2022). If many of the identified genes are co-regulated in a modular way, potentially only a few are functionally relevant for the resistance phenotype.

Cytochrome P450s have been studied extensively for their involvement in insecticide resistance in many pests as they are notorious for their ability to metabolize a varied set of endogenous compounds, phytochemicals, and other xenobiotics like pesticides (Dermauw et al., 2020; Feyereisen, 2006). Moreover, numerous studies were able to link the overexpression of P450s to host plant changes, to exposure to specific phytochemicals and pesticides, and to multi-resistant phenotypes (Dermauw et al., 2013; Feyereisen, 2012; Vandenhole et al., 2021). In our study, several GO terms indicated the importance of P450s in Q_oI resistance. Moreover, many members of the CYP392 family were amongst the highest upregulated genes. *CYP392D2* was extremely overexpressed when comparing FP9 to LON. Likewise, recent studies on resistance of *T. urticae* to the METI-II acaricide cyenopyrafen and the mitochondrial ATP synthase inhibitor fenbutatin oxide have identified *CYP392D2* as the highest overexpressed P450 gene (De Beer et al., 2022; Khalighi et al., 2016). In addition, Dermauw et al. (2013) could link high overexpression levels of *CYP392D2* to the acaricide multi-resistance phenotype in two different *T. urticae* strains and to host plant transfer. Unfortunately, it has not been possible to functionally express member of the CYP392D family. However, other overexpressed P450s such as CYP392E10, CYP392A11 and CYP392A16 were functionally characterized before and were shown to metabolize spirodiclofen/spiromesifen, cyenopyrafen/fenpyroximate and abamectin, respectively (Demaeght et al., 2013; Riga et al., 2015; Riga et al., 2014). Another member of the CYP392 family, *CYP392A11*, displayed extreme levels of overexpression in strain FP9 and is thus an excellent candidate for functional validating. *CYP392A11* has been

shown to strongly respond to acaricide selection before, with high upregulation in response to cyenopyrafen (Khalighi et al., 2016). Riga et al. (2015) have shown that it is able to metabolize cyenopyrafen and fenpyroximate. Here, we show that incubation of bifenazate with CYP392A11 leads to NADPH-dependent substrate depletion, accompanied by the formation of a main metabolite. Further analysis with high resolution LC-MS/MS confirmed ring hydroxylation of bifenazate (**Fig. 6**). Thus, CYP392A11 metabolism likely results in bifenazate detoxification, although the differential toxicity of metabolite and bifenazate awaits further toxicological analysis. Unfortunately, we were unable to test acequinocyl metabolism, as the analytical method for quantification was not reproducible in our hands.

In contrast to the detoxification potential of the P450 family, functional insights on the SDR family are scarce. Nevertheless, SDR enzymes like *tetur06g04970* are amongst the highest overexpressed genes in present and previous studies. Overexpression of *tetur06g04970* has been observed in three resistant *T. urticae* strains that commonly show cross-resistance to pyridaben (Dermauw et al., 2013; Khalighi et al., 2016). SDR enzymes are NAD(P)(H)-dependent oxidoreductases with an average length of only 250-300 amino acids (see InterPro domain IPR020904), and belong to the very large and diverse SDR superfamily. A full survey the SDR superfamily in *T. urticae* by Snoeck et al. (2018) identified not less than 88 full-length SDR's in the *T. urticae* genome, of which several were differentially expressed upon acclimation to various hosts (Snoeck et al., 2018). The actual mechanisms by which the SDR enzymes could be linked to detoxification of xenobiotics or general stress responses, and thus their contribution to resistance in *T. urticae,* remains to be uncovered. Nevertheless, we can hypothesize that SDRs are involved in metabolization of acequinocyl via the reduction of the quinone-group. This hypothesis is based on one of the best known examples where the function of SDR in detoxification of phytochemicals was studied, i.e. in the luna moth, *Actias luna*, where they are known to act via quinone reduction (Lindroth, 1991).

In conclusion, the incidence of known *cytb* target site mutations in European field populations of *T. urticae* appears to be low. During the screening, a new target site mutation, L258F, was identified in a population resistant to both acequinocyl and bifenazate. The observed resistance phenotype appeared to be the result of a complex interplay between the target-site mutation and increased detoxification, involving CYP392A11, which was found to metabolize bifenazate.

5 Acknowledgements

XL is the recipient of a doctoral grant from China Scholarship Council (CSC). This work was supported by the Research Council (ERC) under the European Union's Horizon 2020 research and innovation program, grants 772026-POLYADAPT to TVL and 773902–SUPERPEST to TVL and JV. We thank Eva Skoufa for initial toxicity experiments.

6 Declaration of Competing Interest

The authors declare that they have no conflicts of interest.

7 References:

Anders, S., Pyl, P. T., and Huber, W., 2015 **HTSeq—a Python framework to work with high-throughput sequencing data**. *Bioinformatics,* 31, 166-169, https://doi.org/10.1093/bioinformatics/btu638.

Andrews, S., 2010 **FastQC: a quality control tool for high throughput sequence data**. Babraham Bioinformatics, Babraham Institute, Cambridge, United Kingdom,

Bajda, S., Dermauw, W., Panteleri, R., Sugimoto, N., Douris, V., Tirry, L., Osakabe, M., Vontas, J., and Van Leeuwen, T., 2017 **A mutation in the PSST homologue of complex I (NADH: ubiquinone oxidoreductase) from *Tetranychus urticae* is associated with resistance to METI acaricides**. *Insect Biochem. Mol. Biol.,* 80, 79-90, https://doi.org/10.1016/j.ibmb.2016.11.010.

Bartlett, D. W., Clough, J. M., Godwin, J. R., Hall, A. A., Hamer, M., and Parr‐Dobrzanski, B., 2002 **The strobilurin fungicides**. *Pest Manage. Sci.: Fomerly Pestic. Sci.,* 58, 649-662, https://doi.org/10.1002/ps.520.

Bellina, R. F., and Fost, D. L., 1977 **Acaricidal and aphicidal 2-higher alkyl-3-hydroxy-1, 4-naphthoquinone carboxylic acid esters**. *German Patent DE,* 641, 343.

Benjamini, Y., and Hochberg, Y., 1995 **Controlling the false discovery rate: a practical and powerful approach to multiple testing**. *J. R. Stat. Soc. B,* 57, 289-300, https://doi.org/10.1111/j.2517-6161.1995.tb02031.x.

Caboni, P., Sarais, G., Melis, M., Cabras, M., and Cabras, P., 2004 **Determination of acequinocyl and hydroxyacequinocyl on fruits and vegetables by HPLC-DAD**. *J. Agric. Food Chem.,* 52, 6700-6702, https://doi.org/10.1021/jf0487304.

D'Souza, A. R., and Minczuk, M., 2018 **Mitochondrial transcription and translation: overview**. *Essays Biochem.,* 62, 309-320, https://doi.org/10.1042/EBC20170102.

David, M. D., 2021 **The potential of pro‐insecticides for resistance management**. *Pest Manage. Sci.,* 77, 3631-3636, https://doi.org/10.1002/ps.6369.

De Beer, B., Villacis-Perez, E., Khalighi, M., Saalwaechter, C., Vandenhole, M., Jonckheere, W., Ismaeil, I., Geibel, S., Van Leeuwen, T., and Dermauw, W., 2022 **QTL mapping suggests that both cytochrome P450-mediated detoxification and target-site resistance are involved in fenbutatin oxide resistance in *Tetranychus urticae***. *Insect Biochem. Mol. Biol.,* 145, 103757, https://doi.org/10.1016/j.ibmb.2022.103757.

Dekeyser, M. A., 2005 **Acaricide mode of action**. *Pest Manage. Sci.: Fomerly Pestic. Sci.,* 61, 103-110, https://doi.org/10.1002/ps.994.

Demaeght, P., Dermauw, W., Tsakireli, D., Khajehali, J., Nauen, R., Tirry, L., Vontas, J., Lümmen, P., and Van Leeuwen, T., 2013 **Molecular analysis of resistance to acaricidal spirocyclic tetronic acids in *Tetranychus urticae*: CYP392E10 metabolizes spirodiclofen, but not its corresponding enol**. *Insect Biochem. Mol. Biol.,* 43, 544-554, https://doi.org/10.1016/j.ibmb.2013.03.007.

Dermauw, W., Van Leeuwen, T., and Feyereisen, R., 2020 **Diversity and evolution of the P450 family in arthropods**. *Insect Biochem. Mol. Biol.,* 127, 103490, https://doi.org/10.1016/j.ibmb.2020.103490.

Dermauw, W., Wybouw, N., Rombauts, S., Menten, B., Vontas, J., Grbić, M., Clark, R. M., Feyereisen, R., and Van Leeuwen, T., 2013 **A link between host plant adaptation and pesticide resistance in the polyphagous spider mite *Tetranychus urticae***. *Proc. Natl. Acad. Sci. U. S. A.,* 110, E113-E122, https://doi.org/10.1073/pnas.1213214110.

Di Rago, J. P., and Colson, A. M., 1988 **Molecular basis for resistance to antimycin and diuron, Q-cycle inhibitors acting at the Qi site in the mitochondrial ubiquinol-cytochrome c reductase in *Saccharomyces cerevisiae***. *J. Biol. Chem.,* 263, 12564-12570, https://doi.org/10.1016/S0021-9258(18)37792-5.

Di Rago, J. P., Coppee, J. Y., and Colson, A. M., 1989 **Molecular basis for resistance to myxothiazol, mucidin (strobilurin A), and stigmatellin: cytochrome b inhibitors acting at the center o of the mitochondrial ubiquinol-cytochrome c reductase in *Saccharomyces cerevisiae***. *J. Biol. Chem.,* 264, 14543-14548, https://doi.org/10.1016/S0021-9258(18)71712-2.

Dobin, A., Davis, C. A., Schlesinger, F., Drenkow, J., Zaleski, C., Jha, S., Batut, P., Chaisson, M., and Gingeras, T. R., 2013 **STAR: ultrafast universal RNA-seq aligner**. *Bioinformatics,* 29, 15-21, https://doi.org/10.1093/bioinformatics/bts635.

Feyereisen, R., 2006 **Evolution of insect P450**. Portland Press Ltd., https://doi.org/10.1042/BST0341252.

Feyereisen, R., 2012 **Insect CYP genes and P450 enzymes**. *In* "Insect molecular biology and biochemistry", pp. 236-316. Elsevier, https://doi.org/10.1016/B978-0-12-384747-8.10008-X.

Feyereisen, R., Dermauw, W., and Van Leeuwen, T., 2015 **Genotype to phenotype, the molecular and physiological dimensions of resistance in arthropods**. *Pestic. Biochem. Physiol.,* 121, 61-77, https://doi.org/10.1016/j.pestbp.2015.01.004.

Flampouri, E., 2021 **Agrochemicals inhibiting mitochondrial respiration: Their effects on oxidative stress**. *In* "Toxicology", pp. 3-10. Elsevier, https://doi.org/10.1016/B978-0-12-819092-0.00001-7.

Fotoukkiaii, S. M., Mermans, C., Wybouw, N., and Van Leeuwen, T., 2020a **Resistance risk assessment of the novel complex II inhibitor pyflubumide in the polyphagous pest *Tetranychus urticae***. *J. Pest Sci.,* 93, 1085-1096, https://doi.org/10.1007/s10340-020-01213-x.

660 Fotoukkiaii, S. M., Tan, Z., Xue, W., Wybouw, N., and Van Leeuwen, T., 2020b **Identification**
661 **and characterization of new mutations in mitochondrial cytochrome b that confer**
662 **resistance to bifenazate and acequinocyl in the spider mite *Tetranychus urticae***.
663 *Pest Manage. Sci.,* 76, 1154-1163, https://doi.org/10.1002/ps.5628.
664 Fotoukkiaii, S. M., Wybouw, N., Kurlovs, A. H., Tsakireli, D., Pergantis, S. A., Clark, R. M.,
665 Vontas, J., and Van Leeuwen, T., 2021 **High-resolution genetic mapping reveals cis-**
666 **regulatory and copy number variation in loci associated with cytochrome P450-**
667 **mediated detoxification in a generalist arthropod pest**. *PLoS Genet.,* 17, e1009422,
668 https://doi.org/10.1371/journal.pgen.1009422.
669 Georghiou, G. P., 1969 **Genetics of resistance to insecticides in houseflies and mosquitoes**.
670 *Exp. Parasitol.,* 26, 224-255, https://doi.org/10.1016/0014-4894(69)90116-7.
671 Grosscurt, A., and Avella, L., 2005 **Bifenazate, a new acaricide for use on ornamentals in**
672 **Europe and Africa**. *In* "Proceedings of the BCPC International Congress—Crop
673 Science and Technology", pp. 49-56,
674 Hall, T. A., 1999 **BioEdit: a user-friendly biological sequence alignment editor and analysis**
675 **program for Windows 95/98/NT**. *In* "Nucleic Acids Symp. Ser.", Vol. 41, pp. 95-98.
676 [London]: Information Retrieval Ltd., c1979-c2000.,
677 Hammock, B. D., and Soderlund, D. M., 1986 "**Chemical strategies for resistance**
678 **management**," National Academy Press, Washington, D.C.,
679 https://doi.org/10.17226/619.
680 Jeppson, L. R., Keifer, H. H., and Baker, E. W., 1975 "**Mites injurious to economic plants**,"
681 University of California Press, Berkeley and Los Angeles, California,
682 https://doi.org/10.1525/9780520335431.
683 Khajehali, J., Van Nieuwenhuyse, P., Demaeght, P., Tirry, L., and Van Leeuwen, T., 2011
684 **Acaricide resistance and resistance mechanisms in *Tetranychus urticae* populations**
685 **from rose greenhouses in the Netherlands**. *Pest Manage. Sci.,* 67, 1424-1433,
686 https://doi.org/10.1002/ps.2191.
687 Khalighi, M., Dermauw, W., Wybouw, N., Bajda, S., Osakabe, M., Tirry, L., and Van Leeuwen,
688 T., 2016 **Molecular analysis of cyenopyrafen resistance in the two-spotted spider**
689 **mite *Tetranychus urticae***. *Pest Manage. Sci.,* 72, 103-112,
690 https://doi.org/10.1002/ps.4071.
691 Khalighi, M., Tirry, L., and Van Leeuwen, T., 2014 **Cross-resistance risk of the novel**
692 **complex II inhibitors cyenopyrafen and cyflumetofen in resistant strains of the**
693 **two-spotted spider mite *Tetranychus urticae***. *Pest Manage. Sci.,* 70, 365-368,
694 https://doi.org/10.1002/ps.3641.
695 Khambay, B. P., Batty, D., Beddie, D. G., Denholm, I., and Cahill, M. R., 1997 **A new group**
696 **of plant-derived naphthoquinone pesticides**. *Pestic. Sci.,* 50, 291-296,
697 https://doi.org/10.1002/(SICI)1096-9063(199708)50:4<291::AID-PS604>3.0.CO;2-8.
698 Kim, S. I., Koo, H.-N., Choi, Y., Park, B., Kim, H. K., and Kim, G.-H., 2019 **Acequinocyl**
699 **resistance associated with I256V and N321S mutations in the two-spotted spider**
700 **mite (Acari: Tetranychidae)**. *J. Econ. Entomol.,* 112, 835-841,
701 https://doi.org/10.1093/jee/toy404.
702 Koura, Y., Kinoshita, S., Takasuka, K., Koura, S., Osaki, N., Matsumoto, S., and Miyoshi, H.,
703 1998 **Respiratory inhibition of acaricide AKD-2023 and its deacetyl metabolite**. *J.*
704 *Pestic. Sci.,* 23, 18-21, https://doi.org/10.1584/jpestics.23.18.
705 Kurlovs, A. H., De Beer, B., Ji, M., Vandenhole, M., De Meyer, T., Feyereisen, R., Clark, R.
706 M., and Van Leeuwen, T., 2022 **Trans-driven variation in expression is common**
707 **among detoxification genes in the extreme generalist herbivore *Tetranychus urticae***.
708 *PLoS Genet.,* 18, e1010333, https://doi.org/10.1371/journal.pgen.1010333.

Ladoukakis, E. D., and Zouros, E., 2017 **Evolution and inheritance of animal mitochondrial DNA: rules and exceptions**. *J. Biol. Res.-Thessalon.,* 24, 1-7, https://doi.org/10.1186/s40709-017-0060-4.

Li, H., Handsaker, B., Wysoker, A., Fennell, T., Ruan, J., Homer, N., Marth, G., Abecasis, G., and Durbin, R., 2009 **The sequence alignment/map format and SAMtools**. *Bioinformatics,* 25, 2078-2079, https://doi.org/10.1093/bioinformatics/btp352.

Lindroth, R. L., 1991 **Differential toxicity of plant allelochemicals to insects: roles of enzymatic detoxication systems**. *In* "Insect-plant interactions", pp. 1-34. CRC press, https://doi.org/10.1201/9780203711699.

Love, M. I., Huber, W., and Anders, S., 2014 **Moderated estimation of fold change and dispersion for RNA-seq data with DESeq2**. *Genome Biol.,* 15, 1-21, https://doi.org/10.1186/s13059-014-0550-8.

Lümmen, P., 2007 **Mitochondrial electron transport complexes as biochemical target sites for insecticides and Acaricids**. *In* "Insecticides design using advanced technologies", pp. 197-215. Springer, https://doi.org/10.1007/978-3-540-46907-0_8.

Mota-Sanchez, D., and Wise, J. C., 2022 **Arthropods resistant to Pesticides Database (ARPD)**.

Njiru, C., Xue, W., De Rouck, S., Alba, J. M., Kant, M. R., Chruszcz, M., Vanholme, B., Dermauw, W., Wybouw, N., and Van Leeuwen, T., 2022 **Intradiol ring cleavage dioxygenases from herbivorous spider mites as a new detoxification enzyme family in animals**. *BMC Biol.,* 20, 1-23, https://doi.org/10.1186/s12915-022-01323-1.

Ochiai, N., Mizuno, M., Mimori, N., Miyake, T., Dekeyser, M., Canlas, L. J., and Takeda, M., 2007 **Toxicity of bifenazate and its principal active metabolite, diazene, to *Tetranychus urticae* and *Panonychus citri* and their relative toxicity to the predaceous mites, *Phytoseiulus persimilis* and *Neoseiulus californicus***. *Exp. Appl. Acarol.,* 43, 181-197, https://doi.org/10.1007/s10493-007-9115-9.

Riga, M., Bajda, S., Themistokleous, C., Papadaki, S., Palzewicz, M., Dermauw, W., Vontas, J., and Van Leeuwen, T., 2017 **The relative contribution of target-site mutations in complex acaricide resistant phenotypes as assessed by marker assisted backcrossing in *Tetranychus urticae***. *Sci. Rep.,* 7, 1-12, https://doi.org/10.1038/s41598-017-09054-y.

Riga, M., Myridakis, A., Tsakireli, D., Morou, E., Stephanou, E. G., Nauen, R., Van Leeuwen, T., Douris, V., and Vontas, J., 2015 **Functional characterization of the Tetranychus urticae CYP392A11, a cytochrome P450 that hydroxylates the METI acaricides cyenopyrafen and fenpyroximate**. *Insect Biochem. Mol. Biol.,* 65, 91-99, https://doi.org/10.1016/j.ibmb.2015.09.004.

Riga, M., Tsakireli, D., Ilias, A., Morou, E., Myridakis, A., Stephanou, E. G., Nauen, R., Dermauw, W., Van Leeuwen, T., and Paine, M., 2014 **Abamectin is metabolized by CYP392A16, a cytochrome P450 associated with high levels of acaricide resistance in *Tetranychus urticae***. *Insect Biochem. Mol. Biol.,* 46, 43-53, https://doi.org/10.1016/j.ibmb.2014.01.006.

Robertson, J. L., and Preisler, H. K., 1992 "**Binary response with one explanatory variable**," Chapman and Hall, New York,

Sauter, H., Steglich, W., and Anke, T., 1999 **Strobilurins: evolution of a new class of active substances**. *Angew. Chem., Int. Ed.,* 38, 1328-1349, https://doi.org/10.1002/(SICI)1521-3773(19990517)38:10<1328::AID-ANIE1328>3.0.CO;2-1.

Scheffler, I. E., 2001 **A century of mitochondrial research: achievements and perspectives**. *Mitochondrion,* 1, 3-31, https://doi.org/10.1016/S1567-7249(00)00002-7.

Snoeck, S., Kurlovs, A. H., Bajda, S., Feyereisen, R., Greenhalgh, R., Villacis-Perez, E., Kosterlitz, O., Dermauw, W., Clark, R. M., and Van Leeuwen, T., 2019 **High-resolution QTL mapping in *Tetranychus urticae* reveals acaricide-specific responses and common target-site resistance after selection by different METI-I acaricides**. *Insect Biochem. Mol. Biol.,* 110, 19-33, https://doi.org/10.1016/j.ibmb.2019.04.011.

Snoeck, S., Wybouw, N., Van Leeuwen, T., and Dermauw, W., 2018 **Transcriptomic plasticity in the arthropod generalist *Tetranychus urticae* upon long-term acclimation to different host plants**. *G3: Genes, Genomes, Genet.,* 8, 3865-3879, https://doi.org/10.1534/g3.118.200585.

Sparks, T. C., Crossthwaite, A. J., Nauen, R., Banba, S., Cordova, D., Earley, F., Ebbinghaus-Kintscher, U., Fujioka, S., Hirao, A., and Karmon, D., 2020 **Insecticides, biologics and nematicides: Updates to IRAC's mode of action classification-a tool for resistance management**. *Pestic. Biochem. Physiol.,* 167, 104587, https://doi.org/10.1016/j.pestbp.2020.104587.

Sterck, L., Billiau, K., Abeel, T., Rouze, P., and Van de Peer, Y., 2012 **ORCAE: online resource for community annotation of eukaryotes**. *Nat. Methods,* 9, 1041-1041, https://doi.org/10.1038/nmeth.2242.

Stone, B., 1968 **A formula for determining degree of dominance in cases of monofactorial inheritance of resistance to chemicals**. *Bull. W. H. O.,* 38, 325.

Sugimoto, N., and Osakabe, M., 2019 **Mechanism of acequinocyl resistance and cross-resistance to bifenazate in the two-spotted spider mite, *Tetranychus urticae* (Acari: Tetranychidae)**. *Appl. Entomol. Zool.,* 54, 421-427, https://doi.org/10.1007/s13355-019-00638-w.

Van Leeuwen, T., and Dermauw, W., 2016 **The molecular evolution of xenobiotic metabolism and resistance in chelicerate mites**. *Annu. Rev. Entomol.,* 61, 475-498, https://doi.org/10.1146/annurev-ento-010715-023907.

Van Leeuwen, T., Dermauw, W., Mavridis, K., and Vontas, J., 2020 **Significance and interpretation of molecular diagnostics for insecticide resistance management of agricultural pests**. *Curr. Opin. Insect Sci.,* 39, 69-76, https://doi.org/10.1016/j.cois.2020.03.006.

Van Leeuwen, T., Stillatus, V., and Tirry, L., 2004 **Genetic analysis and cross-resistance spectrum of a laboratory-selected chlorfenapyr resistant strain of two-spotted spider mite (Acari: Tetranychidae)**. *Exp. Appl. Acarol.,* 32, 249-261, https://doi.org/10.1023/B:APPA.0000023240.01937.6d.

Van Leeuwen, T., Tirry, L., and Nauen, R., 2006 **Complete maternal inheritance of bifenazate resistance in *Tetranychus urticae* Koch (Acari: Tetranychidae) and its implications in mode of action considerations**. *Insect Biochem. Mol. Biol.,* 36, 869-877, https://doi.org/10.1016/j.ibmb.2006.08.005.

Van Leeuwen, T., Tirry, L., Yamamoto, A., Nauen, R., and Dermauw, W., 2015 **The economic importance of acaricides in the control of phytophagous mites and an update on recent acaricide mode of action research**. *Pestic. Biochem. Physiol.,* 121, 12-21, https://doi.org/10.1016/j.pestbp.2014.12.009.

Van Leeuwen, T., Van Nieuwenhuyse, P., Vanholme, B., Dermauw, W., Nauen, R., and Tirry, L., 2011 **Parallel evolution of cytochrome *b* mediated bifenazate resistance in the citrus red mite *Panonychus citri***. *Insect Mol. Biol.,* 20, 135-140, https://doi.org/10.1111/j.1365-2583.2010.01040.x.

Van Leeuwen, T., Vanholme, B., Van Pottelberge, S., Van Nieuwenhuyse, P., Nauen, R., Tirry, L., and Denholm, I., 2008 **Mitochondrial heteroplasmy and the evolution of**

insecticide resistance: non-Mendelian inheritance in action. *Proc. Natl. Acad. Sci. U. S. A.,* 105, 5980-5985, https://doi.org/10.1073/pnas.0802224105.

Van Leeuwen, T., Vontas, J., Tsagkarakou, A., Dermauw, W., and Tirry, L., 2010 **Acaricide resistance mechanisms in the two-spotted spider mite *Tetranychus urticae* and other important Acari: a review**. *Insect Biochem. Mol. Biol.,* 40, 563-572, https://doi.org/10.1016/j.ibmb.2010.05.008.

van Lenteren, J. C., Bolckmans, K., Köhl, J., Ravensberg, W. J., and Urbaneja, A., 2018 **Biological control using invertebrates and microorganisms: plenty of new opportunities**. *BioControl,* 63, 39-59, https://doi.org/10.1007/s10526-017-9801-4.

Van Nieuwenhuyse, P., Van Leeuwen, T., Khajehali, J., Vanholme, B., and Tirry, L., 2009 **Mutations in the mitochondrial cytochrome b of *Tetranychus urticae* Koch (Acari: Tetranychidae) confer cross-resistance between bifenazate and acequinocyl**. *Pest Manage. Sci.: Fomerly Pestic. Sci.,* 65, 404-412, https://doi.org/10.1002/ps.1705.

Van Pottelberge, S., Van Leeuwen, T., Khajehali, J., and Tirry, L., 2009a **Genetic and biochemical analysis of a laboratory-selected spirodiclofen-resistant strain of *Tetranychus urticae* Koch (Acari: Tetranychidae)**. *Pest Manage. Sci.: Fomerly Pestic. Sci.,* 65, 358-366, https://doi.org/10.1002/ps.1698.

Van Pottelberge, S., Van Leeuwen, T., Nauen, R., and Tirry, L., 2009b **Resistance mechanisms to mitochondrial electron transport inhibitors in a field-collected strain of *Tetranychus urticae* Koch (Acari: Tetranychidae)**. *Bull. Entomol. Res.,* 99, 23-31, https://doi.org/10.1017/S0007485308006081.

Vandenhole, M., Dermauw, W., and Van Leeuwen, T., 2021 **Short term transcriptional responses of P450s to phytochemicals in insects and mites**. *Curr. Opin. Insect Sci.,* 43, 117-127, https://doi.org/10.1016/j.cois.2020.12.002.

Vlogiannitis, S., Mavridis, K., Dermauw, W., Snoeck, S., Katsavou, E., Morou, E., Harizanis, P., Swevers, L., Hemingway, J., and Feyereisen, R., 2021 **Reduced proinsecticide activation by cytochrome P450 confers coumaphos resistance in the major bee parasite Varroa destructor**. *Proc. Natl. Acad. Sci. U. S. A.,* 118, https://doi.org/10.1073/pnas.2020380118.

Wakasa, F., and Watanabe, S., 1999 **Kanemite (acequinocyl): a new acaricide for control of various species of mites**. *Agrochem. Jpn.,* 75, 17-20.

Wickham, H., 2016 **Data analysis**. *In* "ggplot2", pp. 189-201. Springer, https://doi.org/10.1007/978-3-319-24277-4_9.

Wybouw, N., Kosterlitz, O., Kurlovs, A. H., Bajda, S., Greenhalgh, R., Snoeck, S., Bui, H., Bryon, A., Dermauw, W., and Van Leeuwen, T., 2019 **Long-term population studies uncover the genome structure and genetic basis of xenobiotic and host plant adaptation in the herbivore *Tetranychus urticae***. *Genetics,* 211, 1409-1427, https://doi.org/10.1534/genetics.118.301803.

Xia, D., Yu, C.-A., Kim, H., Xia, J.-Z., Kachurin, A. M., Zhang, L., Yu, L., and Deisenhofer, J., 1997 **Crystal structure of the cytochrome bc1 complex from bovine heart mitochondria**. *Science,* 277, 60-66, 10.1126/science.277.5322.60.

Xue, W., Lu, X., Mavridis, K., Vontas, J., Jonckheere, W., and Van Leeuwen, T., 2022 **The H92R substitution in PSST is a reliable diagnostic biomarker for predicting resistance to Mitochondrial Electron Transport Inhibitors of complex I in European populations of *Tetranychus urticae***. *Pest Manage. Sci.*, https://doi.org/10.1002/ps.7007.

Xue, W., Snoeck, S., Njiru, C., Inak, E., Dermauw, W., and Van Leeuwen, T., 2020 **Geographical distribution and molecular insights into abamectin and milbemectin cross-resistance in European field populations of *Tetranychus urticae***. *Pest Manage. Sci.,* 76, 2569-2581, https://doi.org/10.1002/ps.5831.

857 Xue, W., Wybouw, N., and Van Leeuwen, T., 2021 **The G126S substitution in**
858 **mitochondrially encoded cytochrome *b* does not confer bifenazate resistance in the**
859 **spider mite *Tetranychus urticae***. *Exp. Appl. Acarol.,* 85, 161-172,
860 https://doi.org/10.1007/s10493-021-00668-6.
861 Yang, X. H., and Trumpower, B. L., 1986 **Purification of a three-subunit ubiquinol-**
862 **cytochrome c oxidoreductase complex from *Paracoccus denitrificans***. *J. Biol. Chem.,*
863 261, 12282-12289, https://doi.org/10.1016/S0021-9258(18)67236-9.
864 Yorulmaz Salman, S., and Sarıtaş, E., 2014 **Acequinocyl resistance in *Tetranychus urticae***
865 **Koch (Acari: Tetranychidae): inheritance, synergists, cross-resistance and**
866 **biochemical resistance mechanisms**. *Int. J. Acarol.,* 40, 428-435,
867 https://doi.org/10.1080/01647954.2014.944932.

868

8. Tables

Table 1. Toxicity of acequinocyl and bifenazate to female adults of two *Tetranychus urticae* strains and their crosses

Strain	Acequinocyl				Bifenazate			
	LC_{50} (95% CI) †	**Slope ± SE**	**RR (95% CI)** ‡	**D**§	**LC_{50} (95% CI)**	**Slope ± SE**	**RR (95% CI)**	**D**
LON	9.6 (8.9-10)	4.45±0.33	-	-	1.2 (1.1-1.4)	4.66±0.42	-	-
FP9	2700 (2100-3700)	1.39±0.13	290 (230-360)	-	190 (140-230)	1.85±0.13	150 (130-180)	-
Line 1	50 (41-58)	3.33±0.25	5.2 (4.6-5.9)	-	30 (25-34)	3.04±0.23	25 (22-28)	-
Line 2	60 (54-65)	3.61±0.26	6.2 (5.6-7.0)	-	24 (18-30)	2.72±0.20	20 (17-23)	-
Line 3	67 (61-73)	4.21±0.30	7.0 (6.3-7.8)	-	25 (20-31)	2.81±0.21	21 (18-24)	-
SR (♀ x ♂)	14 (12-17)	2.77±0.25	1.5 (1.3-1.7)	**-0.86**	2.0 (1.6-2.3)	2.90±0.22	1.6 (1.4-1.8)	**-0.81**
RS (♀ x ♂)	130 (110-150)	2.50±0.21	14 (12-16)	**-0.068**	44 (39-48)	5.95±0.57	36 (32-40)	**0.42**

† lethal concentration 50 expressed as mg L^{-1}, with 95% confidence interval (CI)

‡ resistance ratio

§ degree of dominance

875 **Table 2.** Toxicity data of acequinocyl and its active metabolite, acequinocyl-OH, to female adults of two *Tetranychus urticae* strains

Strain	Acequinocyl			Acequinocyl-OH		
	LC_{50}† (95% CI)	Slope ± SE	RR‡ (95% CI)	LC_{50} (95% CI)	Slope ± SE	RR (95% CI)
LON	9.6 (8.9-10)	4.45±0.33	-	1.7 (1.4-1.9)	4.32±0.39	-
FP9	2700 (2100-3700)	1.39±0.13	290 (230-360)	>2000	-	>1200

876 † lethal concentration 50 expressed as mg L^{-1}, with 95% confidence interval (CI)

877 ‡ resistance ratio

878

879

880

881

882

883

884

885

886 **Table 3.** Toxicity of acequinocyl, without and with synergist pretreatment (PBO, DEF, and DEM), to the susceptible LON and the resistant FP9
887 strain of *Tetranychus urticae*.

Synergist	LON			FP9			RR (95% CI)§
	LC_{50} (95% CI)†	Slope (±SE)	SR (95% CI)‡	LC_{50} (95% CI)	Slope (±SE)	SR (95% CI)	
-	11 (10-12)	5.92±0.54	-	2100 (1700-2700)	1.53±0.16	-	200 (160-250)
PBO	11 (10-11)	8.75±0.85	1.0 (0.95-1.1)	190 (170-210)	3.11±0.30	11 (9.0-15)	18 (16-20)
DEF	15 (14-15)	11.6±1.1	0.74 (0.69-0.79)	290 (250-340)	2.48±0.26	7.3 (5.6-9.4)	20 (17-23)
DEM	12 (12-13)	11.2±1.0	0.89 (0.83-0.95)	820 (680-1000)	2.09±0.22	2.6 (2.0-3.4)	67 (58-78)

888 † lethal concentration 50 expressed as mg L^{-1}, with 95% confidence interval

889 ‡ synergism ratio: LC_{50} without synergist relative to LC_{50} with synergist

890 § resistance ratio: LC_{50} of FP9 relative to LC_{50} of LON with the same pretreatment

891

892

893

894

895

896

897

898

899

Table 4. GO enrichment analysis of differentially expressed genes (|Log2FC|>1, BH adjusted p-value < 0.05) in the resistant FP9 strain with ($FP9_{ace}$) or without ($FP9_{unexp}$) exposure to acequinocyl versus the reference strain LON and versus each other.

			$FP9_{unexp}$ vs LON		**$FP9_{ace}$ vs LON**		**$FP9_{ace}$ vs $FP9_{unexp}$**	
Subontology	**GO category**	**Description**	**GeneRatio**	**p.adjust**	**GeneRatio**	**p.adjust**	**GeneRatio**	**p.adjust**
BP	GO:0006508	proteolysis	0.1530	6.2E-14	0.1491	2.10E-12	0	ns
	GO:0050790	regulation of catalytic activity	0.0242	4.3E-08	0.0233	3.33E-07	0	ns
	GO:0055114	oxidation-reduction process	0.1394	5.1E-05	0.1475	1.85E-06	0	ns
	GO:0006869	lipid transport	0.0121	1.3E-03	0.0109	5.15E-03	0	ns
	GO:0008152	metabolic process	0.1273	1.3E-03	0.0140	7.95E-06	0	ns
	GO:0016999	antibiotic metabolic process	0.0121	1.8E-03	0.0140	1.69E-04	0	ns
	GO:0006665	sphingolipid metabolic process	0.0197	1.9E-03	0.0202	1.62E-03	0	ns
	GO:0048477	oogenesis	0.0106	3.5E-03	0.0093	2.04E-02	0	ns
	GO:0005975	carbohydrate metabolic process	0.0500	2.3E-02	0.0543	4.43E-03	0	ns
	GO:0010468	regulation of gene expression	0.0136	4.7E-02	0.0000	ns	0	ns
MF	GO:0008234	cysteine-type peptidase activity	0.0395	2.71E-11	0.0337	7.92E-08	0.0882	2.88E-02
	GO:0005506	iron ion binding	0.0577	4.32E-09	0.0609	3.69E-10	0.1176	2.88E-02
	GO:0016705	oxidoreductase activity, acting on paired donors, with incorporation or reduction of molecular oxygen	0.0459	6.86E-09	0.0457	1.48E-08	0	ns
	GO:0004197	cysteine-type endopeptidase activity	0.0267	1.34E-08	0.0283	2.68E-09	0	ns
	GO:0016758	transferase activity, transferring hexosyl groups	0.0342	1.94E-06	0.0370	8.46E-08	0	ns
	GO:0020037	heme binding	0.0427	1.65E-05	0.0435	1.04E-05	0	ns
	GO:0005319	lipid transporter activity	0.0118	6.11E-04	0.0109	1.87E-03	0	ns
	GO:0031409	pigment binding	0.0107	8.19E-04	0.0130	1.07E-05	0.1765	2.31E-09
	GO:0004348	glucosylceramidase activity	0.0139	1.35E-03	0.0141	9.18E-04	0	ns
	GO:0004252	serine-type endopeptidase activity	0.0342	5.47E-03	0.0304	4.84E-02	0	ns
	GO:0016491	oxidoreductase activity	0.0588	1.08E-02	0.0652	3.92E-04	0	ns
	GO:0016702	oxidoreductase activity, acting on single donors with incorporation of molecular oxygen, incorporation of two atoms of oxygen	0.0096	1.59E-02	0.0141	1.35E-05	0.0882	1.19E-03

GO:0008233	peptidase activity	0.0118	3.35E-02	0.0152	5.97E-04	/	/
GO:0036094	small molecule binding	0	ns	0.0076	1.19E-02	0.1765	6.91E-10
GO:0043169	cation binding	0	ns	0.0185	4.82E-02	0	ns
GO:0004869	cysteine-type endopeptidase inhibitor activity	0	ns	0.0588	2.88E-02	0	ns
GO:0042302	structural constituent of cuticle	0	ns	0.0588	4.52E-02	0.0588	4.52E-02

902

903

9 Figure captions:

Figure 1. Geographical distribution of the surveyed *Tetranychus urticae* field populations in Europe and observed cytochrome *b* target-site resistance mutations. Additional details can be found in Table S1

Figure 2. A) Alignment of the amino acid sequences of the Q_o site of cytochrome *b* from nine organisms. Accession numbers: spider mites *Tetranychus urticae* (EU345430) and *Panonychus citri* (HM367068), the fruit fly *Drosophila melanogaster* (CAB91062), the bird *Gallus gallus* (AAO44995), human *Homo sapiens* (AAX15094), the plant *Arabidopsis thaliana* (CAA47966), the protozoan parasite *Plasmodium falciparum* (NP_059668), the yeast *Saccharomyces cerevisiae* (ABS28693) and the ascomycete fungus *Venturia inaequalis* (AAC03553). Amino acids that are identical or similar are shaded with black or gray, respectively. Triangles above the sequences represent the location of point mutations related to Q_o inhibitor resistance in spider mites. The square represents the mutation investigated in present study. **B)** Summary of validated *cytb* mutations in Q_o sites that are associated with acequinocyl and bifenazate resistance in spider mites. The substitution combination investigated in present study is underlined. °, this mutation was initially reported as I256V combined with N321S (N321S not in the Q_o pocket). *, G126S mutation alone is a neutral mutation for Q_oI resistance, but its contribution in mutation combinations is as yet unknown. Additional information related to phenotypic strength, reciprocal crosses, and congenic lines can be found in Table S5

Figure 3. Acequinocyl and bifenazate concentration-mortality curves of parental crosses and repeated backcrossing experiments. **A)** Acequinocyl data for LON (Susceptible reference), FP9 (Resistant strain), LON♀ × FP9♂ cross (SR), and FP9♀ × LON♂ cross (RS). The corrected mortality of the backcrossed strain RS R ((FP9♀ × LON♂) × FP9♂) is also shown, together with the theoretical concentration-response curve under the hypothesis of a single nuclear gene **B)** Bifenazate data for LON, FP9 and reciprocal cross strains. **C)** Acequinocyl toxicity data for three near-isogenic lines harboring the cytochrome *b* mutation combination G126S + L258F, and the parental strains LON and FP9. **D)** Bifenazate toxicity data for three near-isogenic lines and their parental strains

Figure 4. Transcriptome analysis of the acequinocyl resistant strain FP9 with/without continuous selection pressure. **A)** Principal component analysis (PCA) based on the gene expression profiles of the susceptible reference strain LON, the acequinocyl-selected FP9 strain under continuous acequinocyl exposure ($FP9_{ace}$) and the FP9 strain without acequinocyl

exposure ($FP9_{unexp}$). PC1 and PC2 are represented on the x- and y-axis, respectively, with the percentage of variance explained by each PC shown in parenthesis. **B)** Venn diagram representing the overlap of differentially expressed genes (|Log2FC| > 1, Benjamini Hoghberg adjusted p-value < 0.05) between LON, $FP9_{ace}$ and $FP9_{unexp}$. Indicated in red are the upregulated genes (Log2FC > 1), while downregulated genes (Log2FC < -1) are shown in blue. **C)** Volcano plot indicating differentially expressed genes (|Log2FC| > 1, Benjamini Hoghberg adjusted p-value < 0.05) between $FP9_{unexp}$ and LON. **D)** Scatterplot of the shared differentially expressed genes (|Log2FC| > 1, Benjamini Hoghberg adjusted p-value < 0.05) between $FP9_{ace}$ and $FP9_{unexp}$. In panel C and D, differentially expressed genes belonging to detoxification or transporter gene families (ABCs, CYPs, CCEs, DOGs, GSTs, MFS, SDRs, or UGTs) are color-coded according to the legend

Figure 5. Metabolism of bifenazate by CYP392A11. **A)** HPLC chromatogram of control reactions in the absence of an NADPH regenerating system, displaying no change of the initial bifenazate compound after 2 hours of incubation (eluting at 4.9 min). **B)** HPLC chromatogram showing NADPH-dependent bifenazate depletion (eluting at 4.9 min) and the parallel formation of one unknown metabolite, the metabolite M1 (eluting at 4.075 min)

Figure 6. Parallel reaction monitoring of protonated bifenazate (upper panel) and its metabolite M1, proposed to be hydroxyl-bifenazate (lower panel). Suggested chemical structures of product ions for bifenazate precursor (A. m/z 170.0969 and B. m/z 198.0926) and possible hydroxylation sites shown by product ions of the metabolite-M1 precursor (C. m/z 186.0922 and D. m/z 214.0873). Hydroxylation results in a mass difference of +16 Da between the parental bifenazate and its metabolite M1. This is reflected in the bifenazate (A and B) and M1 metabolite (C and D) product ions formed by collision induced dissociation as they have a 16 Da difference ($A \xrightarrow{+16} C$, $B \xrightarrow{+16} D$), supporting that hydroxylation occurs on the aromatic ring system.

Figure S1. A. Extracted ion chromatograms for ions with m/z values of 301.1549 and 317.1496, obtained using high resolution full scan MS, corresponding to bifenazate and its metabolite produced by CYP392A11, respectively. Upper panel: After 2 hours of incubation of bifenazate (eluting at 3.49 min) in the absence of an NADPH regenerating system. Lower panel: After 2 hours of incubation of bifenazate in the presence of an NADPH regenerating system, demonstrating the formation of metabolite M1 (eluting at 2.61 min). **B.** Accurate mass spectra obtained using HPLC-electrospray ionization. Upper panel: High-resolution mass of protonated

bifenazate at m/z 301.1549. Lower panel: High-resolution mass of the protonated bifenazate metabolite M1 at m/z 317.1496. Also shown are the assigned elemental composition and the corresponding mass accuracy in ppm.

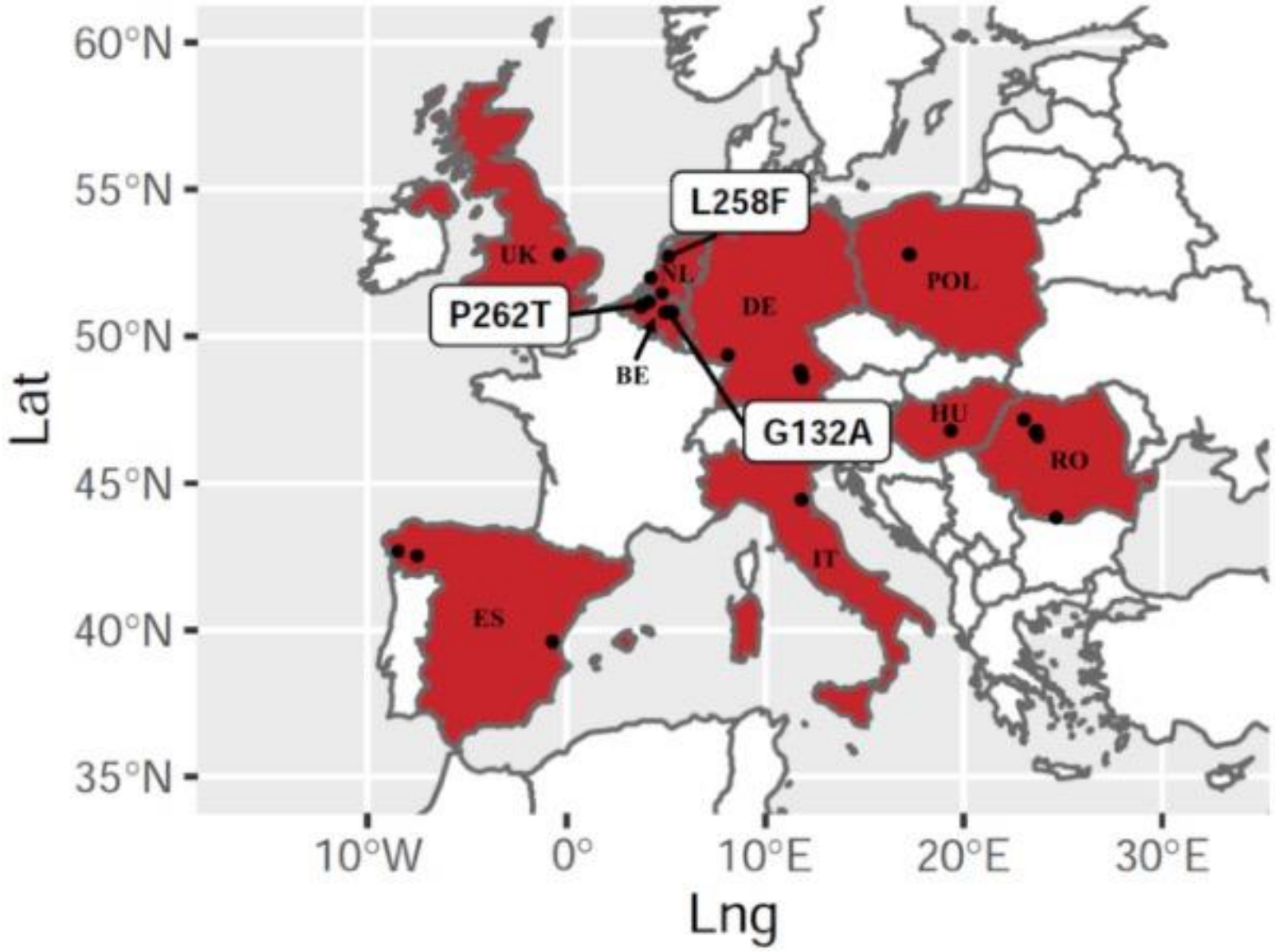
60°N
55°N
50°N
45°N
40°N
35°N
Lat
10°W
0°
10°E
20°E
30°E
Lng
L258F
P262T
G132A
UK
NL
BE
DE
POL
HU
RO
IT
ES

971

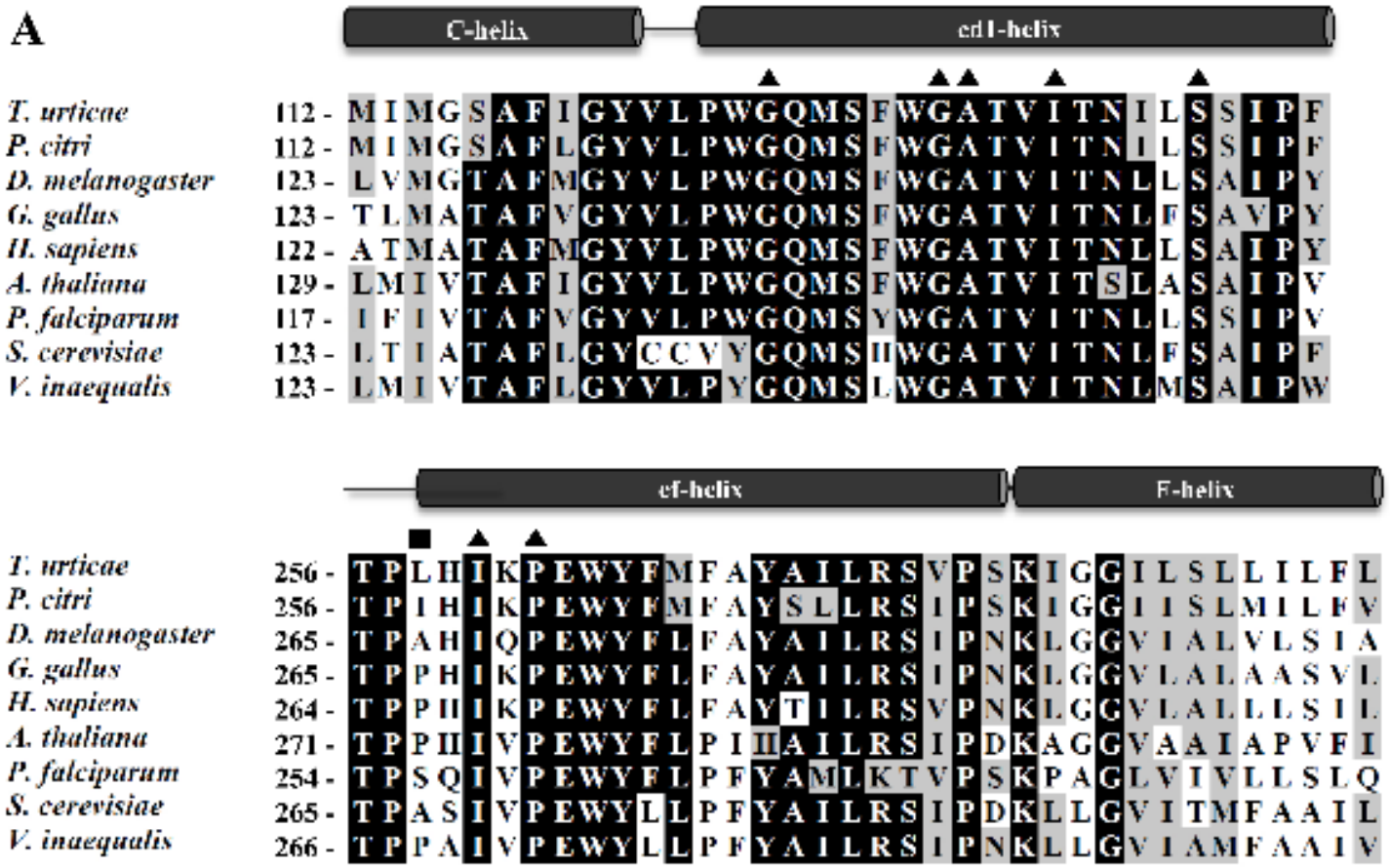
A
C-helix
cd I-helix
T. urticae 112 - M I M G S A F I G Y V L P W G Q M S F W G A T V I T N I L S S I P F
P. citri 112 - M I M G S A F L G Y V L P W G Q M S F W G A T V I T N I L S S I P F
D. melanogaster 123 - L V M G T A F M G Y V L P W G Q M S F W G A T V I T N L L S A I P Y
G. gallus 123 - T L M A T A F V G Y V L P W G Q M S F W G A T V I T N L F S A V P Y
H. sapiens 122 - A T M A T A F M G Y V L P W G Q M S F W G A T V I T N L L S A I P Y
A. thaliana 129 - L M I V T A F I G Y V L P W G Q M S F W G A T V I T S L A S A I P V
P. falciparum 117 - I F I V T A F V G Y V L P W G Q M S Y W G A T V I T N L L S S I P V
S. cerevisiae 123 - L T I A T A F L G Y C C V Y G Q M S I W G A T V I T N L F S A I P F
V. inaequalis 123 - L M I V T A F L G Y V L P Y G Q M S L W G A T V I T N L M S A I P W
ef-helix
F-helix
T. urticae 256 - T P L H I K P E W Y F M F A Y A I L R S V P S K I G G I L S L L I L F L
P. citri 256 - T P I H I K P E W Y F M F A Y S L L R S I P S K I G G I I S L M I L F V
D. melanogaster 265 - T P A H I Q P E W Y F L F A Y A I L R S I P N K L G G V I A L V L S I A
G. gallus 265 - T P P H I K P E W Y F L F A Y A I L R S I P N K L G G V L A L A A S V L
H. sapiens 264 - T P P H I K P E W Y F L F A Y T I L R S V P N K L G G V L A L L L S I L
A. thaliana 271 - T P P H V P E W Y F L P I H A I L R S I P D K A G G V A A I A P V F I
P. falciparum 254 - T P S Q I V P E W Y F L P F Y A M L K T V P S K P A G L V I V L L S L Q
S. cerevisiae 265 - T P A S I V P E W Y L L P F Y A I L R S I P D K L L G V I T M F A A I L
V. inaequalis 266 - T P P A I V P E W Y L L P F Y A I L R S I P N K L L G V I A M F A A I V
B
T. urticae
G126S* + A133T
G126S* + I136T
G126S* + S141F
G126S* + L258F
G132A
I260V° + N326S°
P262T
P. citri
G126S + A133T

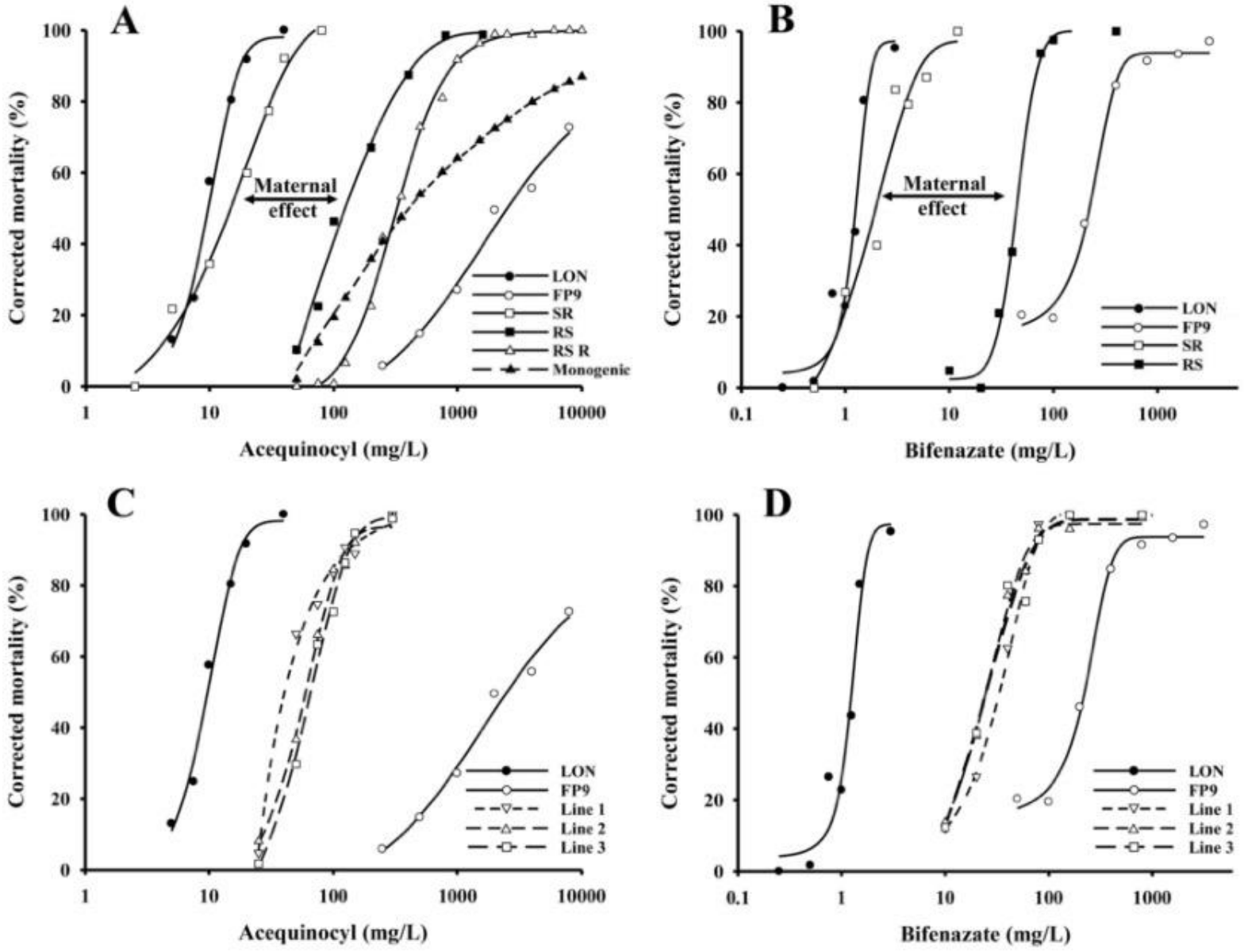
A
Corrected mortality (%)
Maternal effect
LON
FP9
SR
RS
RS R
Monogenic
Acequinocyl (mg/L)
B
Corrected mortality (%)
Maternal effect
LON
FP9
SR
RS
Bifenazate (mg/L)
C
Corrected mortality (%)
LON
FP9
Line 1
Line 2
Line 3
Acequinocyl (mg/L)
D
Corrected mortality (%)
LON
FP9
Line 1
Line 2
Line 3
Bifenazate (mg/L)

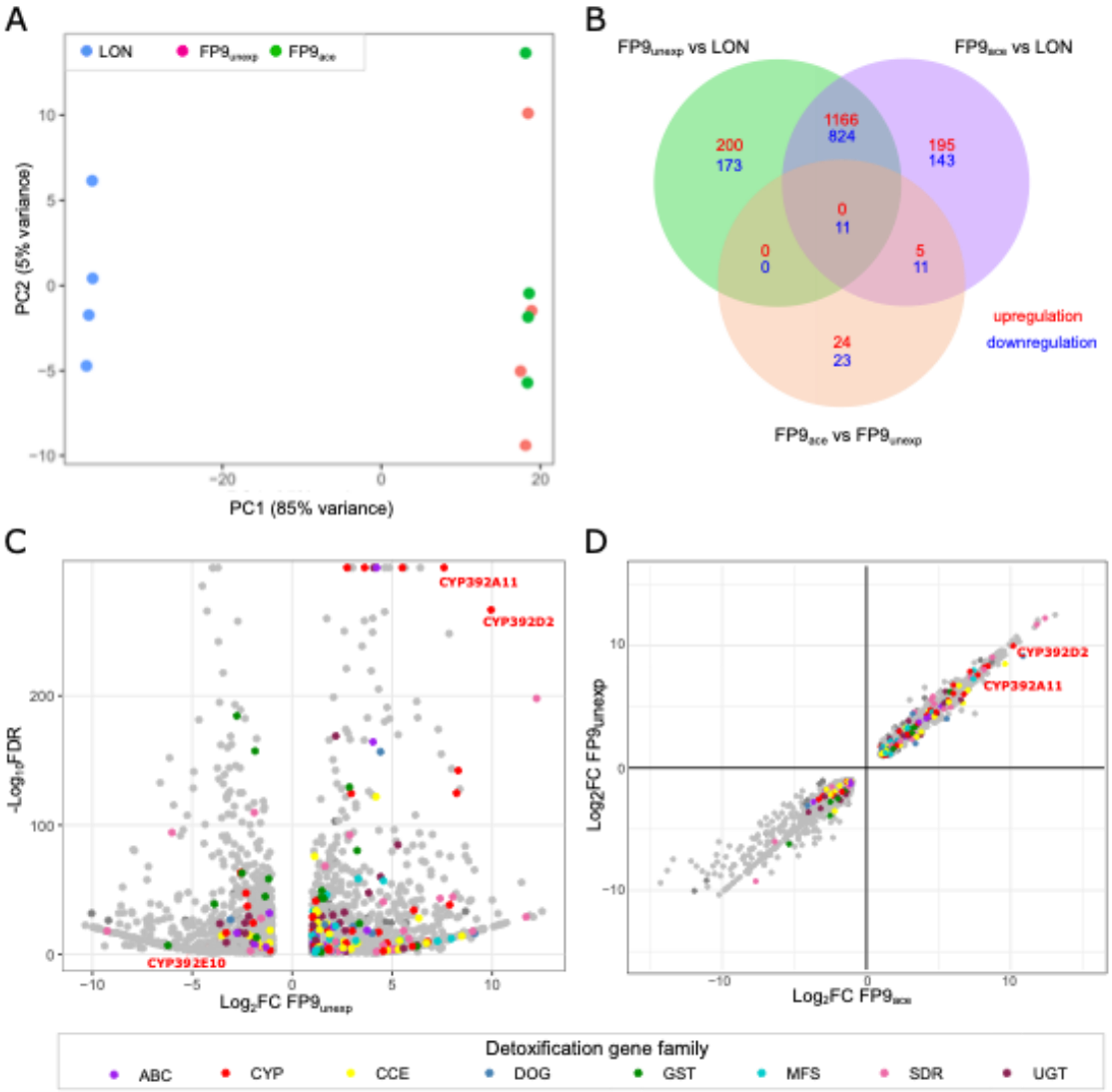
A
LON
FP9unexp
FP9ace
PC2 (5% variance)
PC1 (85% variance)
B
FP9unexp vs LON
FP9ace vs LON
FP9ace vs FP9unexp
200
173
1166
824
195
143
0
11
0
0
5
11
24
23
upregulation
downregulation
C
CYP392A11
CYP392D2
CYP392E10
-Log10FDR
Log2FC FP9unexp
D
CYP392D2
CYP392A11
Log2FC FP9unexp
Log2FC FP9ace
Detoxification gene family
ABC
CYP
CCE
DOG
GST
MFS
SDR
UGT

974

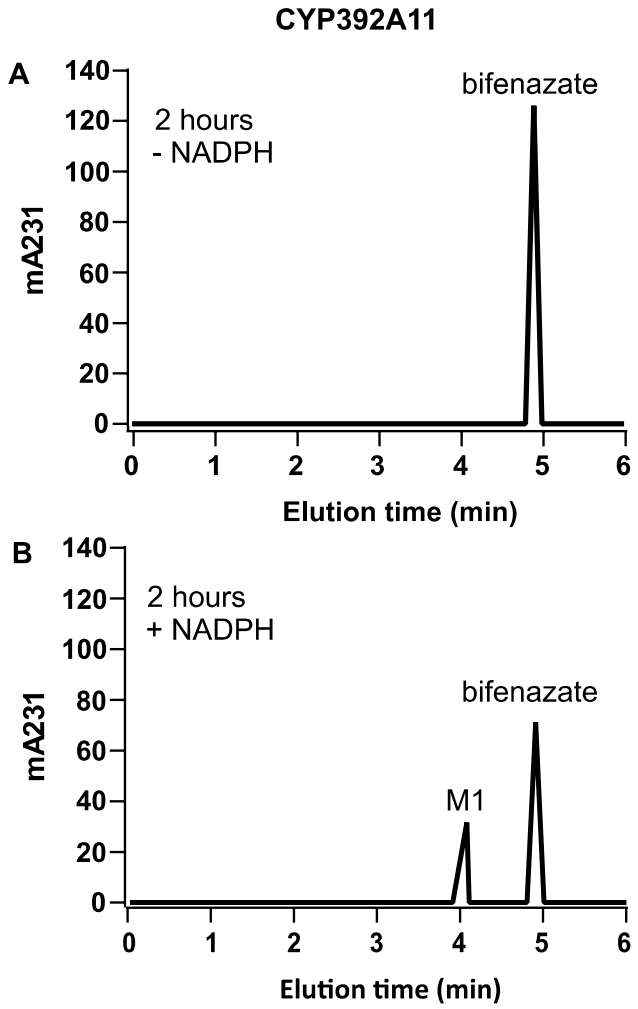
CYP392A11
A
2 hours
- NADPH
bifenazate
mA231
Elution time (min)
B
2 hours
+ NADPH
bifenazate
M1
mA231
Elution time (min)

975

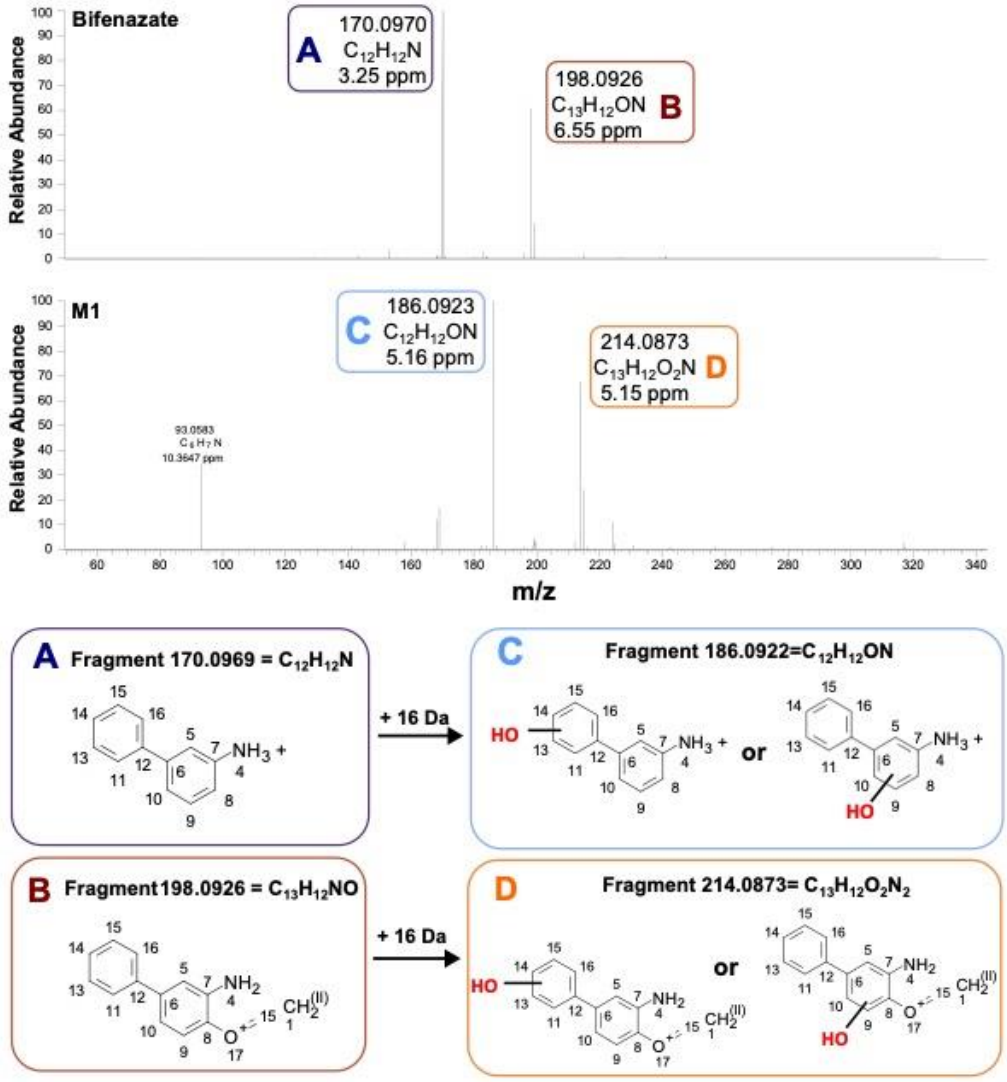
Bifenazate
Relative Abundance
A
170.0970
C12H12N
3.25 ppm
198.0926
C13H12ON B
6.55 ppm
M1
Relative Abundance
C
186.0923
C12H12ON
5.16 ppm
214.0873
C13H12O2N D
5.15 ppm
93.0583
C6H7N
10.3647 ppm
m/z
A Fragment 170.0969 = C12H12N
+ 16 Da
C Fragment 186.0922=C12H12ON
or
B Fragment198.0926 = C13H12NO
+ 16 Da
D Fragment 214.0873= C13H12O2N2
or